https://doi.org/10.5194/essd-2022-311
Preprint. Discussion started: 27 September 2022

Open Access Earth System Science Data Discussions

A comprehensive multidecadal glacier inventory dataset for the Chandra-Bhaga Basin, Western Himalaya, India

Sarvagya Vatsal[1], Anshuman Bhardwaj[2], Mohd Farooq Azam[3], Arindan Mandal[4], Alagappan Ramanathan[1], Ishmohan Bahuguna[5], N. Janardhana Raju[1], Sangita Singh Tomar[6]

[1] School of Environmental Sciences, Jawaharlal Nehru University, New Delhi, 110067, India
[2] School of Geosciences, University of Aberdeen, King's College, Aberdeen, AB24 3FX, United Kingdom
[3] Department of Civil Engineering, Indian Institute of Technology Indore, Simrol, 453552, India
[4] Interdisciplinary Centre for Water Research, Indian Institute of Science, Bengaluru, 560012, India
[5] Space Application Centre, Ahmedabad, 380015, India
[6] Department of Geography, Norwegian University of Science and Technology, Trondheim, No-7491, Norway

Correspondence to: Sarvagya Vatsal (sarvagyavatsaljnu@gmail.com)

Abstract

Delineation of Glaciers is a challenging task in the Himalaya due to its complex topography, cloud cover, seasonal snow cover, hillshade, debris cover. Glacio-hydrological studies including mass balance, run-off, and dynamic modelling rely on the availability of consistent and reliable glacier inventory datasets. This article on data set presents a homogenous, multidecadal inventory of glaciers in the Chandra-Bhaga Basin (CB Basin), western Himalaya, for 1993, 2000, 2010, and 2019. Landsat Thematic Mapper (TM), Enhanced Thematic mapper (ETM+), and Operational Land Imager (OLI) imageries, with minimum snow and cloud cover have been used for enhanced accuracy and consistency. Uncertainty assessment for the generated glacier inventory was performed, following various approaches such as buffer method, standard error estimation, and manual digitisation error and the maximum uncertainty has been quantified. We have identified and manually mapped a total of 251 glaciers with an area > 0.5 km^2, and in order to minimise the uncertainty, field surveys were carried out on 6 glaciers in the basin. Out of these 251 glaciers, 217 are clean ice and 35 were debris-covered glaciers. The estimated total glacier area was 996 ± 62 km^2 in 1993 that decreased to 973 ± 70 km^2 in 2019. Apart from quantifying temporal changes in glacier area, this inventory further allows the estimation of supraglacial debris cover and glacier volume. The supraglacial debris cover area has increased by 14.1 ± 2.54 km^2 (15.2 %) during 1993-2019. Accuracy of the debris cover dataset estimated using ground surveys is 82 % with a kappa coefficient of 0.87. Moreover, a glacier ice volume dataset was also generated by incorporating the inventory into Glacier Bed Topography Version 2 (GlabTop2) model and shows a total of 112.5 ± 41 km^3 of ice volume stored in the CB Basin glaciers. For accuracy assessment of the DEMs generated using ASTER Stereopairs images, DGPS surveys were carried out on (28 GCPs) and off (6 GCPs) the glaciers. Glacier volume uncertainty with respect to the generated DEMs and model bias is 5.3 km^3 and 35.5 km^3 respectively. Overestimation of glacier volume due to over deepening is estimated to be 1.2 km^3. The impact of climate change on the Himalayan glaciers is a matter of serious concern and such holistic multitemporal inventory datasets can help quantify that impact with improved certainty.

https://doi.org/10.5194/essd-2022-311
Preprint. Discussion started: 27 September 2022

1. Introduction

Major river systems including Ganges, Brahmaputra, Indus, Yangtze, and Yellow rivers originate from the Hindu-Kush Karakoram Himalayan (HKKH) region, otherwise known as The Third Pole or Water Tower of Asia (Immerzeel et al., 2010; Viviroli et al., 2011). Himalayan glaciers have been retreating and losing mass under the changing climate (Brun et al., 2017; Shean et al., 2020; Shekhar et al., 2017), and posing a significant threat to regional water security (Azam et al., 2021; Immerzeel et al., 2020; Singh et al., 2016). Glacier inventories serve as a baseline for assessing climate change impacts (Vaughan et al., 2013) via estimation of mass balances (Brun et al., 2017; Kääb et al., 2012a; Shean et al., 2020), hydrological modelling (Bliss et al., 2014; Kraaijenbrink et al., 2017), glacier modelling (Huss and Hock, 2015), volume estimation (Farinotti et al., 2019), and surface velocity (Dehecq et al., 2019; Sam et al., 2016; Sam et al., 2018). The available inventories of Himalayan-Karakoram region (e.g., Bolch et al., 2012; Cogley, 2011; Kääb et al., 2012b; Nuimura et al., 2015) show large discrepancies in the estimated glacierised areas varying between 36,000 to 50,800 km^2, making it difficult to ascertain the glacier-related changes in the region (Azam et al., 2021). Glacier outlines with less uncertainty and having multitemporal coverage aid in the assessment of key glacier properties. Freely accessible glacier outline datasets have opened up several research avenues in spite of considerable variability in accuracy within HKKH (Chowdhury et al., 2021; Mölg et al., 2018). These include the Glacier Area Mapping for Discharge from Asian Mountains (GAMDAM) (Sakai, 2018), Randolph Glacier Inventory (RGI) (RGI Consortium, 2017), and the International Centre for Integrated Mountain Development (ICIMOD) (Barjarcharya and Shreshta, 2011) glacier inventories. RGI and GAMDAM inventories have trumped previously available inventories and enabled access to improved, as well as quality-controlled data which is being used extensively in glacier studies (Brun et al., 2017; Shean et al., 2020; Vijay and Braun, 2016). Moreover, RGI is continually updated by incorporating glacier outlines from other inventories including GAMDAM. In spite of these developments, several studies have investigated the constraints of achieving accurate glacier inventories (Paul et al., 2013, 2015, 2017) and found inconsistency in the glacier outlines of different inventories (Mölg et al., 2018; Sakai, 2018). Main reasons for these inconsistencies are: 1) different reference data (based on data availability, i.e., weather not interfering), 2) steep accumulation area, 3) attached snow field, dead ice, or rock glaciers, 4) location of drainage derived from Digital Elevation Models (DEMs), and 5) supraglacial debris cover (Bhambri and Bolch, 2009; Pfeffer et al., 2014). For the Himalayan glaciers, debris cover is a major challenge in glacier inventory compilation (Mölg et al., 2018; Paul et al., 2013), particularly in the western Himalaya where debris cover is estimated to be ~21 % of the total glacier area (Scherler et al., 2011a). Apart from debris cover, complex geomorphology also contributes to uncertainty in glacier delineation (Bhambri and Bolch, 2009; Bhardwaj et al., 2014). A lack of multitemporal outlines is another limitation of the available inventories, understandably because of their large spatial extent.

Considering the aforementioned challenges and drawbacks of available inventories for studying a given glacierised basin, the present work aims at developing a multitemporal glacier inventory which overcomes these limitations, and further helps investigate the state of glaciers on a multitemporal scale in Chandra-Bhaga Basin (CB Basin), a large glacierised region located in the western Himalaya. Glaciers in CB Basin are some of the most studied ones in the Himalaya (Angchuk et al., 2021; Garg et al., 2017; Kumar et al., 2016; Mandal et al., 2020; Pandey et al., 2017) given the hydrological significance of CB Basin. Chandra and Bhaga rivers, originating from CB Basin are tributaries of Chenab River which on average, has snow and glacier melt contribution of 49 % in its

https://doi.org/10.5194/essd-2022-311
Preprint. Discussion started: 27 September 2022

annual flow (Singh et al., 1997). It has also been quantified that Chenab Basin's glacier snow and ice melt contribution accounts for ~20 % of the total annual flow of the Upper Indus Basin (Winston et al., 2013). Significant water loss (18 %) during 1984-2012 has taken place in Chandra Basin alone (Tawde et al., 2017). The downstream population is completely dependent on snow and ice melt from the glaciers for irrigation and drinking water purposes (Govt. of HP, 2022). Total hydropower generation potential of Chenab Basin in HP is 3032 MW (Kashyap and Parsheera, 2016). A total of 15 hydropower projects are planned on the Chenab River of which Chhatru, Seli, Sachkhas, Reoli-Dugli, and Purthi are dependent on the Chandra and Bhaga rivers (https://sandrp.files.wordpress.com). Moreover, CB Basin is also susceptible to hydrometeorological disasters as a whole and highly vulnerable to snow avalanches and cloudbursts (Pandey et al., 2015). Previous studies have reported adverse impact of the changing climate on glacier health, with a net glacierised area loss of 2.5 % between 1980 and 2010 for the selected glaciers of CB Basin (Pandey and Venkataraman, 2013). The Jankar Chhu Basin, a sub-basin of Bhaga Basin also showed a decrease in area by 7.5 ± 2.2 % during 1971-2016 (Das and Sharma, 2019). Continuous loss of glacier volume increases the uncertainty in water availability for irrigation and hydropower projects (Prakash et al., 2019), thereby highlighting the significance of glacier inventory and ice thickness, volume estimation in the basin as undertaken in the present study.

Glaciers' behavioural response to the changing climate depends on various intrinsic non-climatic factors such as debris cover, aspect, slope, and elevation. A separate consideration of debris cover is important for any glacier inventory in this region, with significant presence of supraglacial debris (Bhardwaj et al., 2015; Garg et al., 2017; Patel et al., 2021; Scherler et al., 2011a; Sharma et al., 2016; Shukla and Garg, 2019), as the presence of supraglacial debris increases the uncertainty in glacier boundary estimation (Frey et al., 2012; Mölg et al., 2018). Supraglacial debris cover is known to affect the rate of ablation (Banerjee and Shankar, 2013; Kääb et al., 2012b; Maurer et al., 2016). Angchuk et al., (2021), Mandal et al., (2020), and Wagnon et al., (2007), using the point-scale ablation data, reported that ablation in debris-covered area was considerably lower as compared to clean ice for Patsio and Chhota Shigri glaciers in CB Basin. Thus, we further aimed at building a dataset of the debris cover area on each glacier for the CB Basin which will aid other researchers in understanding the impact of debris on glacier dynamics in the region.

Glacier inventories also play a crucial role in ice volume estimation. Considering the vulnerability of glaciers in the CB Basin, it becomes important to estimate the ice volume of glaciers and to this end, some in situ observations on select glaciers have been carried out in the CB Basin. Ground Penetrating Radar (GPR) survey conducted on the Chhota Shigri Glacier in 2009 estimated the ice thickness ranging from 124 to 270 m (Azam et al., 2012). For Hamtah and Patsio glaciers, GPR-measured ice thickness ranged from 155 to 247 m (Swain et al., 2018) and 37 to 105 m (Kumari et al., 2021), respectively.

Considering the high glacier density, socio-economic importance, a decreasing trend in precipitation, and an increasing trend in temperature (Bhutiyani et al., 2007, 2010; Li et al., 2018) in the CB Basin, understanding the impact of both climatic- and non-climatic factors on glaciers' area, debris cover change and volume is important. Unfortunately, very limited large scale studies have been conducted in this region with the aim to produce a large scale multitemporal glacier inventory to understand recent basin-wide temporal changes of area and debris cover. To increase the accuracy of glacier-oriented as well as socio-economic impact-based studies at the local and

https://doi.org/10.5194/essd-2022-311
Preprint. Discussion started: 27 September 2022

regional scales, a basin wide glacier inventory is needed in order to: 1) further enhance our existing understanding of the temporal changes in area and debris cover, and 2) provide an estimate of the existing glacier volume in CB Basin. Previously, RGI and GAMDAM inventories were frequently employed in the basin for glacier related studies, but there are some limitations with these inventories, such as: 1) these are not multitemporal inventories, with single glacier outlines derived from the best available data from different years. For example, the RGI inventory is based on satellite data from 1999 to 2010, while GAMDAM is based on data from 1990 to 2010; 2) these inventories are based on semi-automated approaches which is a major source of uncertainty in the delineated glacier outlines for the Himalaya (Bhambri et al., 2011a); 3) no ground surveys have been carried out in the production of these inventories which is yet another source of uncertainty. Thus there is a need to enhance the accuracy, overcome the limitations and to minimise the uncertainty (Shukla et al., 2020), it is necessary for the inclusion of manual digitisation and field-based validation for the generation of glacier inventories, particularly in case on the complex terrain like Himalayan region (Bhambri and Bolch, 2009).

Our study thus presents an extensive inventory of 251 glaciers, covers the entire basin that includes all representative glaciers. Moreover, extensive uncertainty analysis and field validations ensure that the budding/fresh researchers can understand the limitations and adapt and use the dataset as per their requirements, thereby ensuring its wider applicability

Considering the above-mentioned factors, the primary objectives are designed as follows for this study and are defined below:

1- To provide an up-to-date, multitemporal basin-wide inventory of the glaciers in CB Basin,
2- To quantify recent temporal changes in CB Basin glaciers,
3- To quantify the extent of debris cover change in CB Basin glaciers, and
4- To estimate the available ice volume in the glaciers of CB Basin.

2. Study area and data

The CB basin, a sub-basin of the Chenab River (Indus River system), is located in the Lahaul and Spiti district of state HP, India. Lahaul and Spiti is the largest district in the state of HP and accounts for 24.85 % of the state's area (Jreat, 2004). The district recorded a population growth of 6.17 % during 1991-2001. Roughly 8 % of Lahaul and Spiti has scant forest cover, along with willow and poplar plantation-based agroforestry systems in settlement areas, that have, in turn undergone expansion given the population spurt (87.3 % in Jahlmanal watershed alone) during recent decades (Rawat et al., 2010). Major cultivated crops include peas, potato, cauliflower, carrot and barley. For the irrigation of these crops, glacier melt has been used widely mainly through Kuhls and applied through flooding and sprinklers (Govt. of HP, 2022). Apart from this, the state benefits greatly from tourism with the number of yearly visitors increasing rapidly, viz. 161.45 lakhs in 2012-13 to 196.02 lakhs in 2017-18 (Govt. of HP, 2022). Thus, these river systems sustain the population residing both within this basin and downstream as well as the extensive tourist influx, elevating the significance of CB basin as a freshwater reservoir. Geographically, the basin lies in the western Himalayan region, with a total area of ~4120 km^2 (Fig. 1).

https://doi.org/10.5194/essd-2022-311
Preprint. Discussion started: 27 September 2022

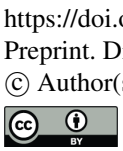

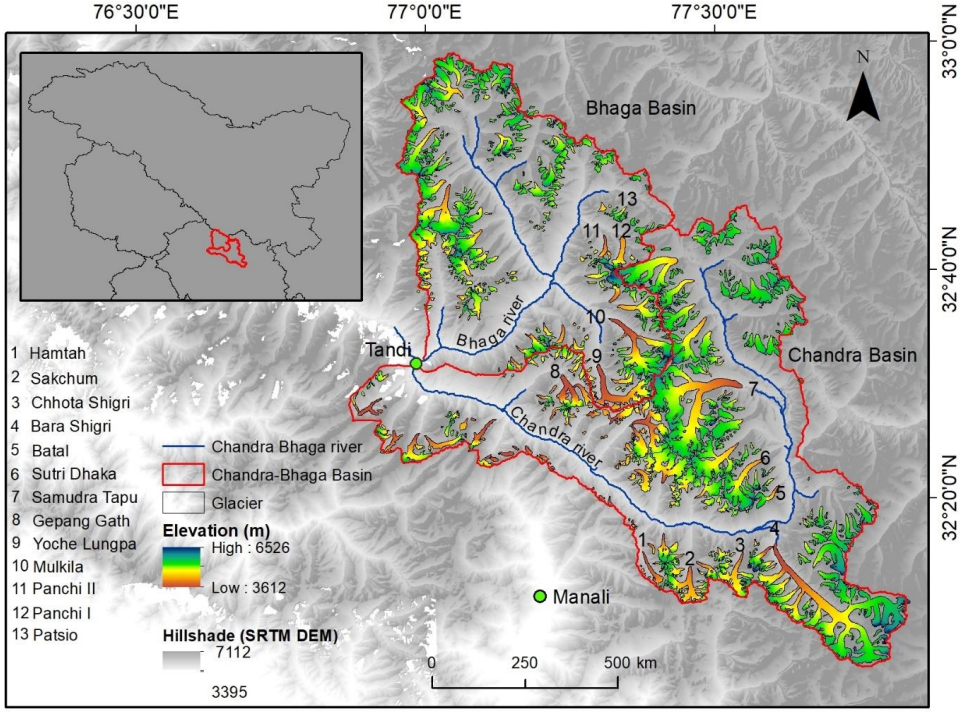

Figure 1. Study area map of the CB Basin. It is located in the Lahaul and Spiti district of state HP, India (inset map) and is part of the western Himalaya. Background image is hillshade using Shuttle Radar Topography Mission (SRTM) DEM. Glacier boundary used is from the present study.

The Chandra and Bhaga rivers originate from the southwest and northwest faces, respectively of the Bara Lacha pass. Chandra River flows for ~125 km and Bhaga for ~80 km to reach their confluence point at Tandi (Fig. 1), southwest of Keylong in the Lahaul and Spiti district of state HP, beyond which the river is named as Chandra-Bhaga or Chenab further downstream in Punjab. The CB Basin lies on the northern ridge of Pir Panjal range with an elevation range of 2400 to 6400 m a.s.l. (Pandey and Venkataraman, 2013). The climate is governed by the Western Disturbances during winter and the Indian Summer Monsoon; thus, the region is characterized as the monsoon-arid transition zone (Bookhagen and Burbank, 2010). Nearly 70 % of annual precipitation occurs in the form of snowfall in winter and rest during summer (Koul and Ganjoo, 2010). CB Basin is heavily glaciated with a glacial area equivalent to 736 km^2 in Chandra and 376 km^2 in Bhaga sub-basins (Prakash and Nagarajan, 2017). For the present study, only glaciers with area greater than 0.5 km^2 have been considered to limit the uncertainty.

2.1 Data sources

Various satellite datasets from different years were used in the present study for glacier boundary delineation and DEM generation (Table S1). Landsat data rectified at the L1 processing level (radiometrically corrected and orthorectified) were used for the glacier inventory delineation while SRTM DEM was used for basin boundary delineation. Different ASTER L1A Reconstructed Unprocessed Instrument Data V003 stereo pairs (ASTER L1A

https://doi.org/10.5194/essd-2022-311
Preprint. Discussion started: 27 September 2022

V003) were used to generate DEMs (details in supplementary material; Table S1). Additionally, very-high resolution images from Google Earth were used to delineate the glacier boundary with minimal uncertainty, especially in the accumulation zone. In two cases, viz. for the years 1993 and 2010; due to unavailability of the cloud-free dataset (less than 15 %) in some regions of the basin, dataset of 1992 and 2011 were used, respectively. RGI 6.0 (RGI Consortium, 2017) and GAMDAM (Sakai, 2018) were used for the comparison with our delineated glacier inventory in the CB Basin. Along with all the satellite datasets, we have also used in-situ glacier thickness dataset derived from GPR survey conducted on Chhota Shigri, Patsio and Hamtah glaciers (Azam et al., 2012; Kumari et al., 2021; Swain et al., 2018). These field observations of glacier thickness were used to validate the Glacier Bed Topography Version 2 (GlabTop2) model and for bias estimation.

3. Methods

The methods used for deriving the glacier inventory, debris cover change and ice thickness datasets have been described at length in the following sections. The associated uncertainty is quantified using various statistical methods as well as field-based observations. Figure 2 shows the brief outline of the workflow.

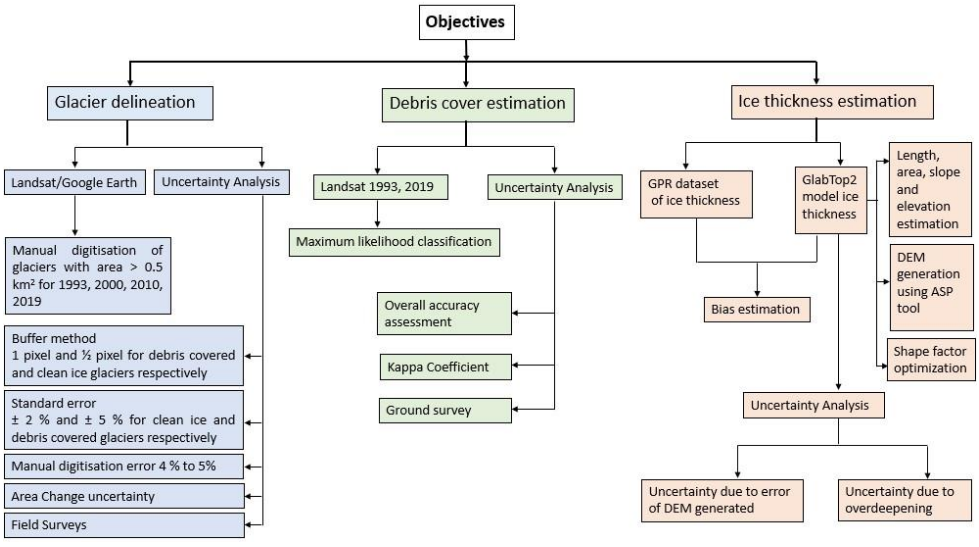

Figure 2. Overview of the workflow adopted for generation of glacier inventory, debris cover and ice thickness dataset.

3.1 Glacier delineation

Different methods for glacier boundary delineation such as band rationing and thresholding were adopted in order to digitise the glaciers (Paul et al., 2004). Supervised classification technique was used for delineation (Aniya et al., 1996; Gratton et al., 1990; Sidjak and Wheate, 1999). Normalised Difference Snow Index (NDSI) was also used for glacier boundary identification (Racoviteanu et al., 2008). The delineation process is challenging for

https://doi.org/10.5194/essd-2022-311
Preprint. Discussion started: 27 September 2022

debris-covered glaciers. Various studies have focused on the automatic delineation of debris-covered glaciers (Bhardwaj et al., 2014; Holobâcă et al., 2021; Mölg et al., 2018). In the present study, all the glaciers with an area > 0.5 km^2 have been studied, which include both clean-ice and debris-covered glaciers. For the Himalayan region, an automated approach is not advisable, as a majority of glaciers have some number of debris cover and very complex geomorphology (Bhambri and Bolch, 2009). It has been assumed that the upper boundary of glaciers has not changed significantly (Bhambri et al., 2011a; Kulkarni et al., 2011). Pan sharpened SWIR-NIR-RED Landsat band combinations have been used. Snouts were identified by the stream origin point and ice wall shadow. Additionally, high-resolution Google Earth images have been used for further verification.

The major challenges for glacier delineation are: 1) debris cover, 2) cloud cover, 3) snow cover, and 4) shadow. Debris cover on the glacier is mainly due to rockfall, avalanche, and steep topography; (Herreid et al., 2015; Scherler et al., 2011b). Debris-covered glaciers can be identified on the basis of certain features such as supraglacial lakes, tallus cone, and arc-shaped ridges (Bodin et al., 2010). Another challenge to glacier delineation is the small solar incidence angle at higher altitudes. To counter these challenges, manual digitisation becomes imperative, ensuring minimum error and better accuracy. To this end, Google Earth imagery was used to further delineate the glacier boundary (Mölg et al., 2018). Minimal interference from cloud cover (less than 15 %) was ensured. To minimise the snow, cover related errors, multiple datasets were downloaded for peak ablation season, viz. June, July, August, September, and October. All the datasets were analysed, and only those images with minimum snow cover on the glacier surface were selected. Another challenge is cast shadow from the mountains which decreases reflectance values. This is a significant problem in high-altitudes regions. To counter these problems, different bands of Landsat were used; and better results were obtained in the blue band combination of Landsat (Paul et al., 2002). Further, as highlighted earlier; Google Earth imagery was also used to improve the accuracy of dataset.

3.2 Debris cover change

Various methods have been applied to identify debris cover change. Unsupervised classification, supervised classification of various input bands, NDSI and Principal Component Analysis (PCA) were used in previous studies (Aniya et al., 1996; Kääb et al., 2002; Racoviteanu et al., 2008; Sidjak and Wheate, 1999). However, we adopt the supervised maximum likelihood classification (MLC) method and applied it to Landsat data with support of the ArcGIS software (Gratton et al., 1990). The MLC method is well established for the Himalayan glaciers with the accuracy of ~ 94 % to 98 % (Yan et al., 2014), while for the Bara Shigri Glacier of CB Basin its accuracy ranges between 82 % to 95 % for the debris cover estimation (Shukla et al., 2009). Further, this method has also been applied to glaciers in regions other than the Himalaya, and accuracy was found to be ~ 90 % (Albert, 2002). A pixel is classified in MLC based on its likelihood of falling into a given class, who's mean, and covariance are described as constituting a normal distribution in the space of multispectral features. Landsat dataset for the year 1993 and 2019 were used (Table S1). For the classification, we generated four training samples, namely snow, ice, ice mix with debris and debris.

3.3 Glacier ice thickness

https://doi.org/10.5194/essd-2022-311
Preprint. Discussion started: 27 September 2022

The glacier ice thickness is estimated using the Glacier Bed Topography2 (GlabTop2) model (Frey et al., 2014). While the Volume and Topography Automation (VOLTA) is another model used for ice thickness estimation (Gharehchahi et al., 2020); we prefer to work with GlabTop2 as it performs better in comparison to VOLTA for the Himalayan region (Zou et al., 2021). This can be attributed to the inclusion of surface morphology of each glacial grid within the GlabTop2 model. Ice thickness is calculated using random pixel cells of DEM within the glacier boundary. The basic assumption is that the thickness of the glacier is zero at its margin. The model works on a grid basis and only two inputs are required, viz. 1) glacier boundary (area, length, slope, minimum and maximum elevation), and 2) DEM. Interpolation of ice thickness from glacier cells was carried out using Inverse Distance Weighing (IDW).

Ice thickness estimation was done along the central flow line of glacier h_f following Eq. (1) from Haeberli and Hoelzle (1995). Parameters of the model are τ, f, r and n, where τ is the function of vertical glacier extent (ΔH) calculated according to Eq. (2) while f is the shape factor and is tuned for the region.

$$h_f = \frac{\tau}{f\rho g sin(\alpha)} \quad (1)$$

$$\tau[kPa] = \begin{cases} 0.5 + 159.8\Delta H - 43.5(\Delta H)^2 : \Delta H \leq 1.6km \\ 150 : \Delta H > 1.6km \end{cases} \quad (2)$$

where h_f is ice thickness along flow line, τ is the average basal shear stress along central flowline, f is the shape factor, ρ is the density of ice, g is gravity, α is the mean surface slope, τ is the function of vertical glacier extent, and ΔH is the glacier extent.

Frey et al. (2014) used a value of f =0.8 for the Chhota Shigri Glacier. In the present study, different model runs were performed using different values of f to understand the best fit for CB Basin glaciers and correspondingly taken as f =0.5. It was observed that r as 0.3 shows the best agreement (Frey et al., 2014). n is the receptivity of the interpolation for ice thickness calculation using a different set of random points, and finally average of n ice thickness is distributed for entire glacier. In this study n is taken as 3. A more detailed description of the model can be found in Frey et al. (2014). The ice thickness estimation from GlabTop2 model was validated against observations from Chhota Shigri, Patsio, and Hamtah glaciers (Table 1).

Table 1. Description of glacier observations used for GlabTop2 model ice thickness validation.

Glacier	Basin	Elevation Range (m a.s.l.)	Area (km^2)	Length (km)	Year	Mean MB (m w.e.)	Reference
Hamtah	Chandra	4050-4650	3.2	5.5	2002-2009, 2010-2012	-1.45	(Azam et al., 2018)
Chhota Shigri	Chandra	4072-5830	15.52	9.0	2002-2019	-0.46±0.40	(Mandal et al., 2020)
Patsio	Bhaga	4875-5718	2.25	2.6	2010-2017	-0.34±0.32	(Angchuk et al., 2021)

There are various other inputs required to run the model. These are: glacier length, area, slope, minimum and maximum elevation, and DEM of the glaciers. The methodology followed for calculation of these inputs is described in the following sections.

https://doi.org/10.5194/essd-2022-311
Preprint. Discussion started: 27 September 2022

3.3.1 Length estimation

An automatic allocation method was deployed to estimate the glacier length along the central line using an algorithm developed by Zhang et al. (2021). The model algorithm works in the Python environment and site package ArcPy of ArcGIS. Model input parameters are: 1) glacier polygon, and 2) DEM. Data used for glacier polygon delineation and DEM should have similar spatial resolution and acquisition year. There are a total of 11 adjustable parameters (P1 – P11) based on the classification of glacier polygon through a set of reasonable rules (refer Table 1 in Zhang et al., 2021). In this algorithm, local highest point of the glacier is affected by the perimeter of the glacier (P_g). We took the given area (A_t) and perimeter (P_t, Eq. 3) of the equilateral triangle corresponding to A_t as grading threshold. According to the area (A_g) and the perimeter (P_g) of each glacier's outer boundary, all the glaciers were divided into different categories (Eq. 4).

$$P_t(A_t) = 2 \times 3^{0.75} \times A_t^{0.5} \tag{3}$$

$$L(A_g, i) = \begin{cases} \boldsymbol{i}: & A_g \in [A_{i-1}, A_i)\ and \\ & P_g \in [P(A_i, +\infty)\ and \\ & i \in (1,5] \\ \boldsymbol{i}: & A_g \in [A_i, A_{i+1}) and \\ & P_g \in \left[P(A_i), P(A_{i+1})\right) and \\ & i \in [1,5] \\ \boldsymbol{i}: & A_g \in [A_{i+1}, A_{i+2}) and \\ & P_g \in \left(0, P(A_{i+1})\right) and \\ & i \in [1,5) \\ 0: & the\ above\ conditions\ are\ not\ met \end{cases} \tag{4}$$

A= {0,1,5,20,50, +∞} is the threshold set of glacier area (km^2) and i= {1,2,3,4,5} is the corresponding level of glaciers and is used as the index of array A. Glaciers are divided into three categories: simple, simple compound, and complex glaciers. Some basic rules are followed in this model for e.g., Equilibrium Line Altitude (*ELA*) is always lower than the local highest point of the glacier, and there is only one snout of the glacier. The readers may refer to Zhang et al., (2021) for a detailed description.

3.3.2 Area, slope and elevation estimation

All other parameters required for the GlabTop2 model are calculated in ArcGIS. The area of all the glaciers is computed using different polygons, which were manually digitised for year 2019. Slope and elevation (minimum and maximum) were calculated from DEMs.

3.3.3 DEM generation

DEMs were generated from the ASTER L1A stereo pairs having cloud cover less than 15 %. The Ames Stereo Pipeline (ASP) v2.6.0 was used to process these ASTER L1A stereo pairs, with the void-filled SRTM-GL1 product serving as a seed DEM for initial orthorectification. With default parameters (7*7 pixel window), the ASP Semi-Global Matching (SGM) correlator (Shean et al., 2016) can improve ASP correlation algorithms for cases with low image resolution. To remove residual artifacts, ASP's default SGM disparity map filters (3*3 pixel median filter and 3*3 pixel texture aware smoothing filter with scaling factor 0.13) were used. The output DEMs

https://doi.org/10.5194/essd-2022-311
Preprint. Discussion started: 27 September 2022

were posted at a spatial resolution of 30 m, with elevations relative to the WGS84 ellipsoid. A 2 pixel erosion of the outer DEM boundaries is applied at the end to remove any lingering edge artifacts. Each one of these ASTER DEMs was co-registered with the reference SRTM DEM to remove all horizontal and vertical offsets. There were identified static control sites, and it was believed that no elevation change would occur at these locations. The Nuth and Kääb (2011) technique was implemented interactively, with robust filtering and outlier removal. The resulting DEMs have some offset in horizontal (x and y) and vertical (z) directions, detailed in the supplementary section (Table S2). All co-registered ASTER DEMs were carefully analysed to find and remove any remaining problematic or low-quality DEMs. For detailed description of ASP, readers are referred to Shean et al. (2016; 2020).

3.4 Uncertainty and accuracy assessments. We have attempted to quantify all the sources of uncertainties related to all three datasets: glacier delineation, debris cover, and ice thickness estimation. To increase the accuracy of the methods followed, we have done field surveys on different glaciers in the CB Basin. The details of processes involved are described in the following sections.

3.4.1 Uncertainty related to glacier delineation

The challenges mentioned in Sect. 3.1 are mainly responsible for uncertainty in glacier delineation. These kinds of uncertainties can be taken care of in the manual digitisation. According to previous studies, there are mainly three kinds of uncertainty related to the glacier delineation. First is the uncertainty of automatically and manually digitised glacier outline which is a fixed uncertainty (Mölg et al., 2018). Second is the buffer-based estimate (Bolch et al., 2010, Granshaw and Fountain, 2006), in which the final uncertainty is determined by the input image's pixel size. Another source of uncertainty is related to the workload (Paul et al., 2017) associated with the manual digitisation of the glaciers.

To encounter all these source of uncertainty, first we applied ± 2 % and ± 5 % uncertainty for the clean ice and debris cover glaciers, respectively, this is an upper boundary estimate, and the overlap between the two surface types is excluded., then we applied buffer method (Granshaw and Fountain, 2006) with ±1/2 pixel and ± 1 pixel for clean-ice and debris-covered glaciers, respectively (Mölg et al., 2018) and at last, to enhance the overall accuracy and quantify the uncertainty because of workload, we have carried out multiple digitisation of the glaciers to estimate the uncertainty and extensive field surveys to validate our manually digitised glacier boundaries and termini positions; discussed in detail in the next section.

3.4.2 Field validation. Rigorous field surveys were carried out on the Hamtah Glacier in August 2017, Chhota Shigri in June and August 2019, Patsio in June and August 2019, Mulkila in June 2017, Yoche Lungpa in June 2017 and on Panchi II Glacier in June and August 2019. It has been observed that Mulkila, Yoche Lungpa, Hamtah and Panchi II glaciers are highly debris covered (Fig. 3).

https://doi.org/10.5194/essd-2022-311
Preprint. Discussion started: 27 September 2022

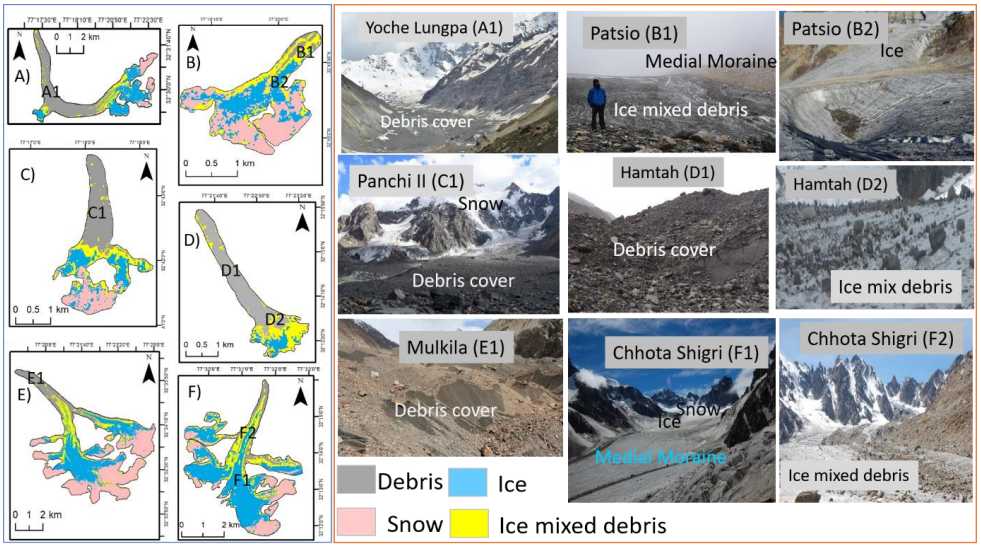

Figure 3. Field photographs (in the right panel) for validation and classified Landsat images showing snow, ice, debris and ice mix debris cover. A) Yoche Lungpa Glacier, B) Patsio Glacier, C) Panchi II Glacier, D) Hamtah Glacier, E) Mulkila Glacier, F) Chhota Shigri Glacier.

We measured the termini/snout position of all the glaciers during our field surveys using handheld Garmin eTrex 30X GPS, which has a position accuracy of ± 3 m (Chowdhury et al., 2021). We also did surveys on the glaciers and surveyed various terminal and lateral moraines, one of the major sources of uncertainty in case of the debris cover glacier boundary identification. These two surveys (termini and moraines) increase the accuracy of our glacier inventory dataset. Apart from this, the accumulation area of Chhota Shigri, Hamtah, Panchi II, and Patsio glaciers were also surveyed in order to enhance the accuracy of the glacier boundary in the accumulation area and to quantify any avalanche related uncertainties in boundary identification. Since all the satellite scenes used in the study are not of the same year, we ensure that scenes are within ± 2 years difference to the target year, such that uncertainty because of this time gap is minimised (Mölg et al., 2018).

Uncertainty in area change was estimated using the following equation (Hall et al., 2003; Wang et al., 2009):

$$U_{area} = 2 \times U_{retreat} \times V \quad (5)$$

Here U_{area} is the uncertainty in the area change estimation, $U_{retreat}$ is the uncertainty in the area estimation, and V is the image pixel resolution.

3.4.3 Accuracy assessment of MLC method for debris cover estimation. Four training classes were defined: a) snow, b) ice, c) ice mixed debris, and d) debris over the glaciers. In order to ensure high accuracy, on-field visual inspection is essential (Paul, 2000). All the training samples were validated by field surveys done on Chhota Shigri, Patsio, Panchi, Mulkila, Hamtah, and Yoche Lungpa glaciers (Fig. 3). Of these, Chhota Shigri and Patsio are almost clean-ice glaciers having 3.4 % and 12 % debris cover of total glacier area (Angchuk et al., 2021; Azam et al., 2016). Ground surveys were carried out for accuracy assessment of the image classification. A total of 154

https://doi.org/10.5194/essd-2022-311
Preprint. Discussion started: 27 September 2022

ground validation points were chosen. The confusion matrix, derived from the image map and classified data; was generated for accuracy assessment (Janssen and van der Wel, 1994). A coefficient of agreement between classified image and ground reference data was calculated using Kappa (Mohd Hasmadi and Kamaruzam, 2008). The value of Kappa lies between 0 and 1, where 1 represents complete agreement between two datasets, and 0 represents agreement due to chance only (Fitzgerald and Lees, 1994). Equations (6) and (7) quantify accuracy and Kappa coefficient.

$$Overall\ accuracy = \frac{Total\ number\ of\ correctly\ classified\ pixels}{Total\ number\ of\ reference\ pixels} \quad (6)$$

$$Kappa\ coefficient = \frac{(TS \times TCS) - (\sum Column\ total \times Row\ total)}{TS^2 - \sum(Column\ total - Row\ total)} \quad (7)$$

where *TS* = total sample, *TCS* = total correctly classified samples

3.4.4 Uncertainty in glacier ice thickness due to the generated DEMs.

Various DEMs were generated to estimate the ice thickness of the glaciers. To quantify the uncertainty related to these generated DEMs, we have performed differential global positioning system (DGPS) survey of various ground control points (GCPs) on the Chhota Shigri, Panchi II and Patsio glaciers at an error less than 1 cm (Preety et al., 2022; Shukla et al., 2020). DGPS was used in static mode to gather a total of 34 GCPs. To harmonise the coordinate system of the DEMs produced, all the GCPs were imported as point vectors and reprojected in the ArcGIS environment. Out of 34 GCPs, 13 points are on Panchi II, 7 points on Patsio and 14 points on the Chhota Shigri glacier, all in the year 2019. Over all sets of the derived elevation estimates, a linear-fit regression analysis was conducted to determine the degree of correlation. We calculated the mean error for all GCPs, mean error and standard deviation, making use of DGPS-based elevation data as the basis for all statistical computations and analysis (Bolkas et al., 2016; Massuel et al., 2022).

3.4.5 Uncertainty in ice thickness due to overdeepening

Glacier bed overdeepening occurs mainly because of the erosive power of the glacier (Linsbauer et al., 2016). Voids in the DEMs generated from ASTER L1A stereo pairs were filled using nearest neighbor interpolation algorithm following IDW interpolation method in ArcGIS (Setianto and Triandini, 2015). To estimate the overdeepening, another DEM (without the glacier ice) was created by subtracting the ice thickness from the DEM (used for ice thickness estimation in the model). Next, the void filled DEM was subtracted from the DEM without glacier ice (Furian et al., 2021; Linsbauer et al., 2016). Various studies have chosen different threshold values of the surface area for computation of overdeepening: 10^4 m^2 (Colonia et al., 2017; Linsbauer et al., 2016), and 10^5 m^2 (Furian et al., 2021). In the present study, we have used an overdeepening threshold of 10^5 m^2 based on a large scale overdeepening study over High Mountain Asia (Furian et al., 2021), wherein lies CB Basin.

4. Results and Discussion

This section is structured as follows: The basic statistics over the domain as estimated from our self-generated inventory are presented in Sect. 4.1, temporal changes in glacier area during 1993-2019 are discussed in Sect. 4.1.1, and uncertainty in glacier delineation is quantified in Sect. 4.1.2. Debris cover change and associated

https://doi.org/10.5194/essd-2022-311
Preprint. Discussion started: 27 September 2022

uncertainties are quantified in Sect. 4.2. Ice thickness and volume estimates along with errors arising from the generated DEM and due to overdeepening are elaborated in Sect. 4.3. Thereafter, comparisons with previous studies in the region follow in Sect. 4.4.

4.1 Basin-wide statistics

We identified 251 glaciers (larger than 0.5 km^2) in the CB Basin. Total glacier area of the 251 glaciers in CB Basin was 973 ± 70 km^2 in 2019. Mean slope for glaciers in the basin is 18 ° while mean elevation ranges from 4796 to 5678 m a.s.l. While the average glacier area in the basin is 3.5 km^2, only 58 out of 251 glaciers have an area greater than 3.5 km^2, implying that most glaciers are smaller in size. 172 glaciers have an area > 1 km^2 while only 16 glaciers have an area > 10 km^2. Bara Shigri is the largest glacier in this basin, with an area of 131.32 ± 9.54 km^2 followed by Samudra Tapu Glacier with an area of 81.68 ± 5.1 km^2. Glaciers having debris cover > 15 % of the total area (on the basis of maximum likelihood classification) are considered as debris covered (Janke et al., 2015) and subsequently, a total of 35 such glaciers have been identified. 11 periglacial lakes were also identified out of which 5 are with clean glaciers and 6 are with debris-covered glaciers. Based on this criterion, out of 251 glaciers; 216 are classified as clean and 35 as debris-covered glaciers.

4.1.1 Glacier area change

Overall, the inventory shows a decline in glacier area from 996 ± 62 km^2 in 1993 to 973 ± 97 km^2 in 2019. Total loss of 2.3 ± 0.08 % is observed in CB Basin. This significant area loss is in turn, adversely affecting the glacier health in the basin. Moreover, the rate of area loss is inconsistent over the studied time period. To further quantify these changes on a decadal basis, 3-time windows have been considered: 1993-2000, 2000-2010, and 2010-2019 (Table S3). The total glacier area was 996 ± 62 km^2 in 1993 which reduced to 989 ± 68 km^2 in 2000 with an average loss of 0.025 km^2 per glacier. In the next decade, i.e., 2000 to 2010, total glacier area decreased further to 982 ± 66 km^2 in 2010 with mean area loss of 0.029 km^2. The total glacier area further shrinked to 973 ± 70 km^2 at the rate of 0.036 km^2 in the recent decade, i.e., 2010-2019. These temporal changes in glacier area vary with respect to glacier size and presence/absence of debris cover as seen in Fig. 4a.

https://doi.org/10.5194/essd-2022-311
Preprint. Discussion started: 27 September 2022

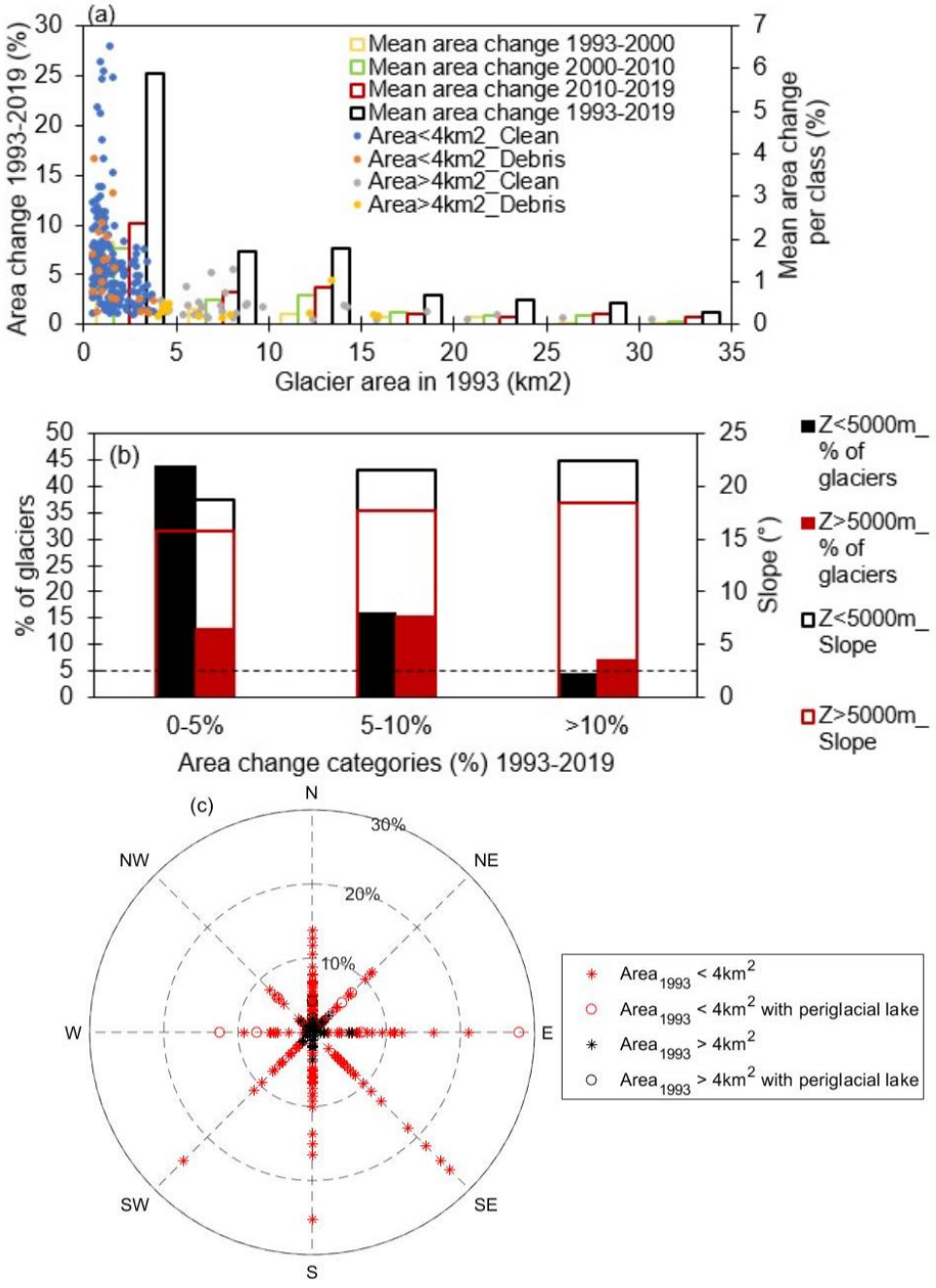

Figure 4. (a) Area change (%) in debris covered and clean ice glaciers plotted as a function of glacier area in 1993 (scatter) and temporal changes (%) in category-wise mean glacier area (column). (b) Percentage of glaciers and

https://doi.org/10.5194/essd-2022-311
Preprint. Discussion started: 27 September 2022

mean slope corresponding to minimum elevation (Z) < or > 5000 and for different area change categories. (c) Aspect and area change (%) for glacier area in 1993 < or > 4 km^2 and presence/absence of periglacial lake.

The columns in Fig. 4a represent the mean area change (%) corresponding to glacier area classes (0-5, 5-10…,30-35 km^2) for different time periods. The mean area change is higher for small glaciers (highest in area class 0-5 km^2) throughout 1993-2019. Intercomparison shows that prominent changes occurred during 2010-2019 as compared to other decades. The effect of presence/absence of debris cover in minimising glacier area loss is also evident from the scatterplot (Fig. 4a). It demarcates glaciers with area > or < 4 km^2 (mean glacier area in 1993). Majority of glaciers (79.68 %) fall below 4 km^2 and the area change is higher in case of clean ice glaciers (max = 27.86 %) compared to debris covered glaciers (max = 16.44 %). Similarly, in case of larger glaciers (> 4 km^2), excluding Samudra Tapu and Bara Shigri glaciers, we find clean ice glaciers (max = 5.38 %) underwent greater area change than debris covered glaciers (max = 4.23 %). Total 216 clean ice and 35 debris-covered glaciers (including the largest glacier in the basin, Bara Shigri) were outlined in our inventory. Total glacier area for clean ice (debris covered) glaciers was 702.4 ± 38 km^2 (293.9 ± 25 km^2) during 1993 and decreased to 682 ± 36 km^2 (290.3 ± 25 km^2) in 2019. Also, the mean glacier area for clean ice (debris covered) glaciers changed from 3.3 (8.16) km^2 in 1993 to 3.17 (8.06) km^2 in 2019. Despite their comparatively smaller numbers, mean glacier area of the debris covered glaciers is greater than clean ice glaciers, which shows greater variability in case of debris covered glaciers (Standard deviation, σ = 21.62) compared to clean ice glaciers (σ = 6.81).

Figure 4b shows the glacier area change with respect to glacier elevation. In the CB Basin, glacier elevation (Z) ranges from 3533 to 5374 m a.s.l and the mean minimum elevation is 4797 m a.s.l. In the minimum elevation range of Z <5000m (Z>5000m), 44% (13%) of total glaciers correspond to an area change of < 5 %, whereas 4.3 % (7.2 %) correspond to > 10% area change between 1993-2019. Mean elevation for the clean ice glaciers was 5251 m a.s.l., while for the debris covered glaciers it was 4956 m a.s.l. We also note that snout elevation of most debris-covered glaciers is low compared to the clean-ice glaciers. The slopes of glaciers in the basin vary from 9 ° to 36 ° with mean slope of ~18 °. Glaciers with area larger (smaller) than the mean glacier area: 4 km^2; had mean slope of 16 ° (20 °), respectively. Irrespective of the elevation range, steeper slopes correspond to greater area change. The glaciers' average slope varies in different areas, for example accumulation area is steep in all glaciers while debris covered areas have gentle slope. Glacier area change is maximum (> 25 %) for glaciers facing South (Southwest- Southeast) (SW-SE) as seen in Fig 4c. In all, 71 glaciers are north facing, 31 northeast, 32 east facing, 25 southeast, 37 south facing, 21 southwest, 15 west facing, and 19 glaciers have a northwest orientation. Average area loss for south (north) facing glaciers was 0.11 ± 0.007 km^2 (0.08 ± 0.004 km^2). However, the highest area change (27.86 %) corresponds to an east facing glacier, which can be attributed to the presence of a periglacial lake at the snout. It is known that heat absorption by the peri-glacial lake water is responsible for glacier mass loss at the snout, contributing towards higher snout retreat (Bolch et al., 2012; King et al., 2018). Total of 11 glaciers with periglacial lakes have been identified. Out of these, 9 were associated with clean ice and 2 with debris covered glaciers. Total area loss of these 11 glaciers was 2.03 ± 0.42 km^2 with the mean area loss of 0.19 ± 0.06 km^2 which is significantly high for such a small number of glaciers. While these losses are likely to increase manifold with the changing climate, every glacier has its own micro-climatic condition (Hannah et al., 2000; Wagner et al., 2019) owing to its morphology, resulting in heterogeneity in the glacier response to climate change. This further

https://doi.org/10.5194/essd-2022-311
Preprint. Discussion started: 27 September 2022

exacerbates the need for comprehensive inventory-debris cover-ice thickness datasets with known uncertainties for glacier monitoring.

4.1.2 Uncertainties in glacier inventory delineation

The resulting uncertainty of the mapped glacier area has been estimated using different approaches. We obtain thresholds of ± 27 and ± 29 km^2 by applying standard uncertainties of 2 % for clean ice and 5 % for debris covered glaciers respectively. Uncertainty estimated using buffer method (½ pixel for clean ice and 1 pixel for debris covered glaciers) ranges between ± 62 to ± 70 km^2. In order to prevent double counting of the overlapping areas of neighboring glaciers, both approaches are used with glacier complexes. Finally, multiple digitisations were carried out which resulted in a ± 4 % standard deviation (averaged over all experiments). This high value shows the mapping challenges in the Himalayas due to cloud, debris, shadow and snow cover as described in Sect. 3.1. We evaluated the uncertainty in the digitisation of small glaciers (less than 1 km^2) that had a significant portion of their surface shrouded in shadow and a considerable portion covered in barely perceptible debris and found it to be ± 6 % of the glacier area mapped. Such cases are extremely rare in our database and have no bearing on the level of uncertainty as a whole. It has been reported previously that analyst interpretation for debris covered glaciers and glacier parts in shadow can differ up to 50 % (Paul et al., 2013, 2015). In the present study, we find that for such glaciers manual digitisation is favorable. We have validated the glacier inventory using field photographs (Fig. 3.) taken for various glaciers and find that the impact of shadow on the digitisation of the accumulation areas and debris covered glaciers is minimised to ~ 16 %. It is totally dependent on the exegesis of the debris cover on the glacier.

To determine the extent of agreement between existing inventories and our glacier inventory, we compared the boundaries of representative glaciers (marked in Fig. 1.) in the CB Basin with those in RGI and GAMDAM inventories. These are shown in Fig. 5.

https://doi.org/10.5194/essd-2022-311
Preprint. Discussion started: 27 September 2022

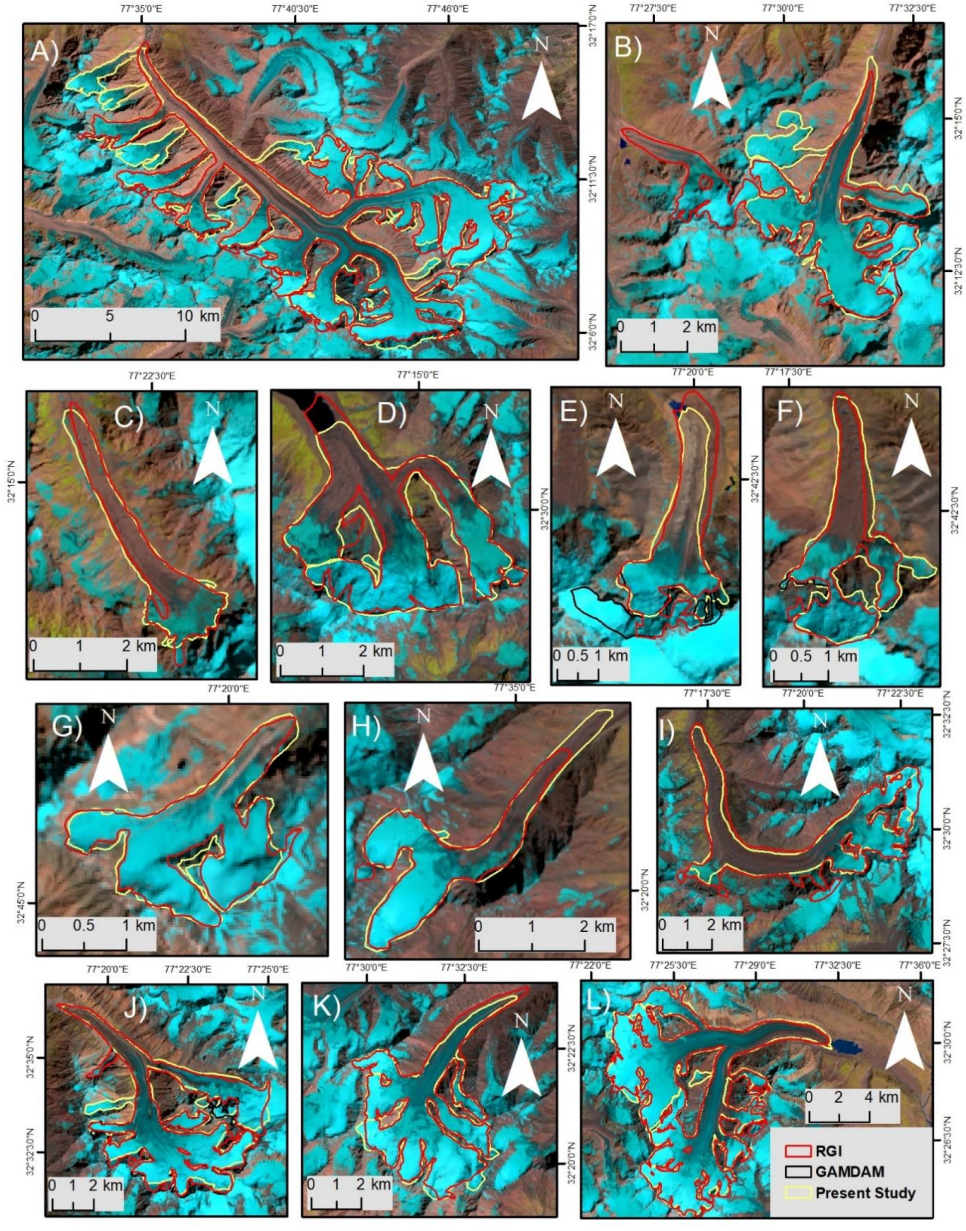

Figure 5. Comparison of RGI, GAMDAM and present inventory for A) Bara Shigri (S.No. 4 in Fig. 1), B) Chhota Shigri (3), C) Hamtah (1), D) Gepang Gath (8), E) Panchi I (12), F), Panchi II (11), G) Patsio (13), H) Batal (5), I) Yoche Lungpa (9), J) Mulkila (10), K) Sutri Dhaka (6), L) Samudra Tapu (7) glaciers. Background image is Landsat 8 composite.

https://doi.org/10.5194/essd-2022-311
Preprint. Discussion started: 27 September 2022

Several issues related to the gap area, differences in mapping methods and skill of the analysts involved lead to misrepresentation and limit the accuracy of inventories, e.g., RGI and GAMDAM overestimate parts of the boundary in some glaciers including, Chhota Shigri (B), Gepang Gath (D), Panchi I (E) and Sutri Dhaka (K) glaciers, while underestimating for others such as Batal (H), Bara Shigri (A), and Panchi II (F). Total glacier area estimated using our glacier inventory is ~ 26 % and 9 % less in comparison to RGI and GAMDAM, respectively for the glaciers of area > 0.5 km^2. It has been observed previously that the RGI inventory has overestimated glacier area by ~100 % in the North Patagonian Andes (Zalazar et al., 2020), ~10 % in China (Li et al., 2022) which may be attributed to uncertainties associated with the misinterpretation of seasonal snow cover and debris cover (Pfeffer et al., 2014). For the entire High Mountain Asia, the overestimation by RGI inventory is ~ 24 % (Nuimura et al., 2015), which confirms our glaciers inventory dataset is well suited for the CB Basin. The effect of debris cover induced uncertainty on glacier delineation is evident while comparing the inventories for the two largest glaciers (>50 km^2) in the CB Basin: Bara Shigri (debris covered) and Samudra Tapu (clean ice). While all 3 inventories (RGI, GAMDAM, present study) estimate an area of ~80 km^2 for Samudra Tapu, the presence of debris cover on Bara Shigri resulted in an underestimation of glacier area by both RGI and GAMDAM (112.35 km^2) compared to present study (131 km^2) and others (Berthier et al., 2007, Schauwecker et al., 2015). Presence of debris at the terminus of many glaciers, is a major constraint to the automated methods of glacier delineation in the CB basin. It has been well established that in the Himalaya, the automated approach is better for clean ice glaciers while manual delineation (as adopted in present study) has been comparatively more accurate for the debris cover glaciers (Bhambri and Bolch, 2009).

4.2 Debris cover change

Debris cover on a glacier affects its melting pattern, velocity and hydrology (Burger et al., 2019; Rounce et al., 2021). As per a study focused on Sakchum, Chhota Shigri, and Bara Shigri glaciers; debris cover has increased by 1.03 km^2, 0.45 km^2, and 4.92 km^2 respectively between 1993 and 2014 (Garg et al., 2017). The distinctions in area change of debris covered and clean ice glaciers in the CB Basin have been discussed in Sect. 4.1.1. Consequently, it becomes important to estimate the temporal change in glacier debris cover. For this, we have used the maximum likelihood classification, and calculated its accuracy following Eqs. (6) and (7).

The total debris cover in CB Basin was 91.4 ± 16.45 km^2 in 1993 that has increased to 105.5 ± 18.9 km^2 in 2019. There is a change of 14.1 ± 2.54 km^2 (15.2 %) debris covered area during this time period. We have provided an up-to-date dataset of the debris cover for all 251 glaciers delineated in the basin, for years 1993 and 2019, which will be the first large scale dataset quantifying debris cover change in CB Basin. This dataset will aid future glacier studies in CB Basin to better understand the impact of debris on glacier dynamics. Further, Table 2 entails the debris cover changes for some representative glaciers (marked in Fig. 1) in the basin.

Table 2. Debris cover (in km^2 and % glacier area) of representative glaciers (marked in Fig. 1.) of the basin for years 1993 and 2019.

S.No. (As in Fig.1)	Glacier	Debris cover (km^2)		Debris cover change (km^2)	Debris cover (% glacier area)	
		1993	2019		1993	2019
1	Hamtah	2.25 ± 0.41	2.32 ± 0.42	0.07 ± 0.01	59	62
2	Sakchum	2.80 ± 0.50	3.80 ± 0.68	1.00 ± 0.18	18	24

https://doi.org/10.5194/essd-2022-311
Preprint. Discussion started: 27 September 2022

3	Chhota Shigri	1.45 ± 0.26	2.16 ± 0.39	0.71 ± 0.13	8	12
4	Bara Shigri	18.46 ± 3.32	23.40 ± 4.21	4.94 ± 0.89	14	18
5	Batal	1.17 ± 0.21	1.19 ± 0.21	0.02 ± 0.004	25	27
6	Sutri Dhaka	0.24 ± 0.04	0.53 ± 0.09	0.29 ± 0.05	1	2
7	Samudra Tapu	5.53 ± 1.01	8.49 ± 1.52	2.96 ± 0.53	6	10
8	Gepang Gath	4.34 ± 0.78	4.47 ± 0.80	0.13 ± 0.03	30	30
9	Yoche Lungpa	6.55 ± 1.17	6.90 ± 1.24	0.35 ± 0.06	42	45
10	Mulkila	3.51 ± 0.63	4.28 ± 0.77	0.77 ± 0.14	11	14
11	Panchi II	1.66 ± 0.30	1.67 ± 0.31	0.01 ± 0.002	39	40
12	Panchi I	1.86 ± 0.33	1.87 ± 0.34	0.01 ± 0.002	42	44
13	Patsio	0.17 ± 0.03	0.17 ± 0.03	0 ± 0	6	6

4.2.1 Uncertainties in estimation of debris covered area

Since we have followed maximum likelihood classification (discussed in Sect. 3.2) for debris-covered area estimation, we quantify the overall accuracy (Eq. 6) and the Kappa coefficient (Eq. 7) discussed in Sect. 3.4.3. To ensure high accuracy, on-field visual inspection is essential (Paul, 2000). All the training samples were validated by field surveys done on Chhota Shigri, Patsio, Panchi, Mulkila, Hamtah, and Yoche Lungpa glaciers (Fig. 3). Total 154 ground observation points were sampled and compared to the remotely classified satellite imageries (Table 3).

Table 3. Accuracy assessment table for the classified image for debris, snow, ice, and ice mix debris classes with ground validation points.

	Field observation				Remotely classified
	Debris	Ice	Debris mix Ice	Snow	
Debris	39	0	2	0	41
Ice	0	44	3	2	49
Debris mix Ice	0	6	27	0	33
Snow	0	2	0	29	31
Total	39	52	32	31	154

The overall accuracy of this classification is found to be 90 %, while individual accuracy was 95 %, 90 %, 94 % and 82 % for debris, ice, snow and ice mix with debris respectively, which is considerably high with respect to the complex geomorphology of the glaciers in the CB Basin. Kappa value is 0.87, which shows good agreement between classified image and ground validation points. Maximum uncertainty was found to be ~18 % for the class debris mix with the ice. To ensure a wide margin of error, we assign this value as the uncertainty in the debris cover area estimation using maximum likelihood classification. Consequently, total uncertainty in debris cover was ± 16.45 km^2 in 1993 and ± 18.9 km^2 in 2019. Uncertainty in the debris cover change was ± 2.54 km^2.

4.3 Glacier ice thickness and volume

GlabTop2 model is used to estimate the thickness of glaciers in the CB Basin. Ramsankaran et al. (2018) used this model to estimate the ice thickness of the Chhota Shigri Glacier. They computed glacier thickness at multiple elevation zones by using different shape factors (*f*) for each elevation zone. Further, Pandit and Ramsankaran (2020) estimated the ice thickness for 65 glaciers of Chandra Basin by developing individual shape factor for every glacier. However, for a large-scale study over the region, these approaches are arduous, time consuming

https://doi.org/10.5194/essd-2022-311
Preprint. Discussion started: 27 September 2022

and require high computing resources which are not readily available. Considering these challenges, it is important to have a common shape factor that is representative of all glaciers in the CB Basin and has minimal uncertainty. With this in mind, we developed a common shape factor for CB Basin glaciers, which will minimise the computation required for ice thickness estimation, while also assuring model accuracy. To ensure this common shape factor's suitability for different types of glaciers, we have validated our model using the observed ice thickness on three glaciers in the CB Basin, viz. Chhota Shigri, Patsio, and Hamtah, which adds to the robustness of the modelled ice thickness dataset. Primary reasons for choosing these 3 set of glaciers for model validation are as follows: 1) Hamtah is a debris-covered glacier while the other two are clean-ice glaciers, 2) Hypsometric analysis (Fig. S1) explains that for Hamtah only 5-10 %, Chhota Shigri 45-50 %, and Patsio 50-55 % of total glacier area is above the mean Equilibrium Line Altitude (ELA) estimated by Angchuk et al., (2021); Mandal et al., (2020); and Pratap et al., (2016), respectively; 3) slopes of ablation area of Hamtah, Chhota Shigri, and Patsio are gentle (6°), moderate (12°) and steep (19°), respectively; 4) Hamtah has an avalanche-fed accumulation (Banerjee and Shankar, 2014), while others are not prone to significant avalanche impact (Azam et al., 2018); 5) elevation range for Hamtah, Chhota Shigri, and Patsio glaciers are 4050-4650, 4072-5830 and 4875-5718 m a.s.l., respectively, and 6) availability of GPR-measured ice thickness dataset for validation. The distinctions between these 3 glaciers ensure that the common shape factor found suitable for all 3 will be well suited for glaciers with a wide range of intrinsic parameters.

4.3.1 Model result and bias estimation

The GlabTop2 model was validated on the basis of observations (in- situ GPR-based ice thickness data) available for Chhota Shigri Glacier for year 2009 (Azam et al., 2012), Hamtah Glacier for year 2012 (Swain et al., 2018), and Patsio Glacier for year 2017 (Kumari et al., 2021) as shown in Fig. 6. The horizontal accuracy of the location of GPR survey points in these studies is ±0.1 m. The respective year's DEMs were generated from ASTER stereo-pair images using ASP (discussed in Sect. 3.3.3).

https://doi.org/10.5194/essd-2022-311
Preprint. Discussion started: 27 September 2022

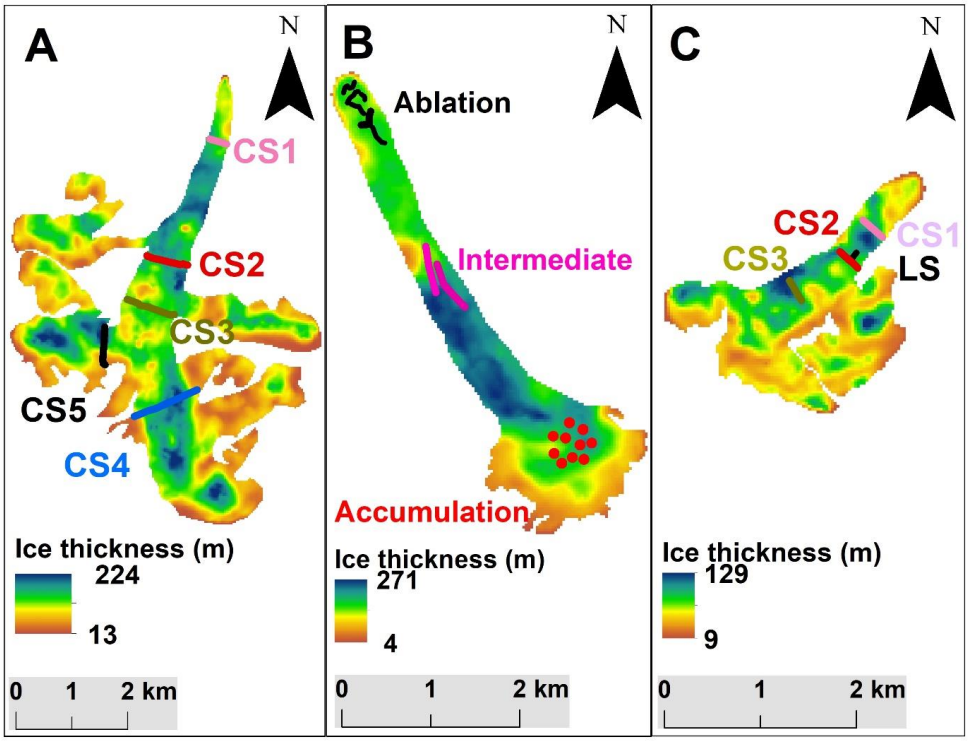

Figure 6. GlabTop2 model thickness comparison for: A) Chhota Shigri, B) Hamtah, and C) Patsio glaciers with different ground validation points. CS1, CS2, CS3, CS4, and CS5 represent different cross-sections of the GPR survey done on the glaciers, while LS refers to the longitudinal section on the Patsio Glacier. For B) Hamtah Glacier, black and pink lines on ablation zone and red dots on accumulation zone are locations of the GPR surveys.

After multiple runs of the model using different shape factors (Table S4), the shape factor value of 0.5 was used for CB Basin glacier thickness estimation. This shape factor model bias ranges from -35 to 39 m which is admissible for basin-scale thickness estimation (Table 4).

Table 4. Model output comparison (Shape factor, $f = 0.5$) with GPR surveys conducted on Chhota Shigri, Patsio, and Hamtah glaciers.

Glacier	Sections	Observation (m)	Model (m)	Bias (m)
Chhota Shigri	CS1	96	135	39
	CS2	197	163	-34
	CS3	163	128	-35
	CS4	208	181	-27
	CS5	136	141	5
Patsio	CS1	37	61	24
	CS2	57	80	-23
	CS3	105	101	-4
	LS	53	78	25
Hamtah	Ablation	155	168	13
	Intermediate	224	208	-16

https://doi.org/10.5194/essd-2022-311
Preprint. Discussion started: 27 September 2022

	Accumulation	247	223	-24

4.3.2 Uncertainty due to the generated DEMs

DGPS surveys conducted on the Chhota Shigri, Patsio and Panchi II glaciers provided elevation of total 34 points, including 28 points on-glacier and 6 points off-glacier. These points were compared with the DEM elevation generated using in glacier volume of ± 5.3 km^3 for CB Basin.

4.3.3 Model error due to overdeepening

As discussed earlier in Sect. 3.4.5, based on a large-scale study conducted by Furian et al., (2021) over the High Mountain Asia (wherein lies the CB Basin), we selected an overdeepening threshold of 10^5 m^2 for this study. On generating the ice free glacier DEM and using an overdeepening threshold of 10^5 m^2 (Furian et al., 2021), we estimate that total overdeepening area in the CB Basin is 10.74 km^2 with a mean depth of 111 m. This results in an overestimation of total ice volume of the basin by 1.19 km^3, which is then subtracted from the total glacier volume to account for the overdeepening.

4.3.4 Total volume of the glaciers

To estimate the thickness of the glaciers in the CB Basin, GlabTop2 was run for the year 2020. However, as no cloud free images for the year 2020 were available for some glaciers (especially in the Jankar Chhu watershed; Fig. 7), DEMs of 2014 were used for ice thickness estimation. Another area for which no dataset was available is around Tandi (the confluence of Chandra and Bhaga rivers, Fig. 1), wherein, also DEMs of 2014 were used. As a result, we could not estimate the ice thickness and volume of the 25 glaciers that fall within this no-data region. Nevertheless, we have covered 914 km^2 of glacier area in the basin, which corresponds to ~93 % of the total glacier area delineated in our study. The ice thickness of glaciers in the basin is shown in Fig. 7.

https://doi.org/10.5194/essd-2022-311
Preprint. Discussion started: 27 September 2022

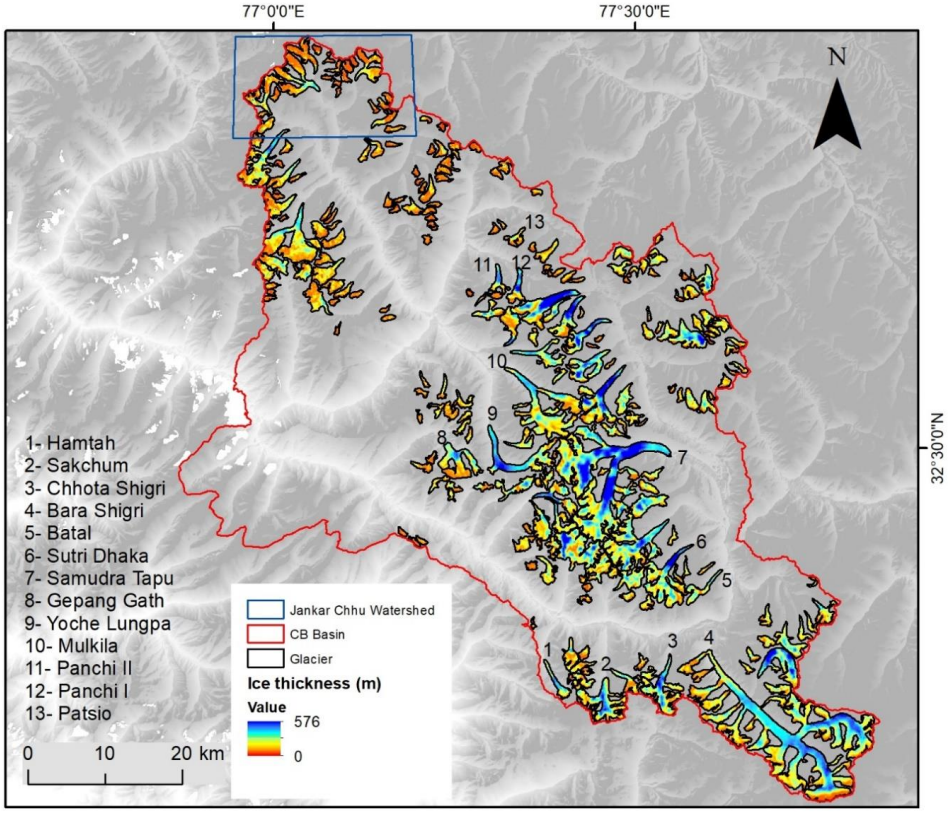

Figure 7. Ice thickness of glaciers in the CB Basin estimated using GlabTop2 model. Background is hill shade of SRTM DEM.

Maximum glacier thickness was found to be 576 ± 45 m for the glacier with RGI ID: RGI 60-14.14970 in the CB Basin. The present study aims to quantify glacier ice thickness and volume at the basin scale, and therefore, estimated the volume of 226 out of 251 delineated glaciers in the CB Basin. After subtracting the overdeepening volume, i.e., 1.19 km^3, and considering the uncertainty in the ice volume estimation because of DEMs generated (± 5.3 km^3), and model bias in ice thickness estimation (± 35.6 km^3), total ice volume of the basin is 112.5 ± 41 km^3. Ice thickness of glaciers in Jankar Chhu watershed (Fig. 8) is relatively lower than other glaciers in the CB Basin. This can be attributed to: 1) mean slope of the Jankar Chhu watershed is 24 ° which is higher in comparison to the mean slope of CB Basin glaciers (18°). Slope is a key factor in glacier ice thickness estimation, higher slope of the glacier will increase the flow of glacier ice which will, in turn increase mass wasting, resulting in reduced ice thickness, 2) glaciers in this watershed are relatively smaller (mean area 1.2 km^2) compared to other glaciers in the basin (mean area 3.5 km^2), and it is already well established that smaller glaciers are more susceptible towards climate change (Azam et al., 2018; Bhambri et al., 2011b; Chand and Sharma, 2015), 3) majority of the glaciers in the Jankar Chhu watershed have southern orientation. It is known that southern facing glaciers face more radiation flux compared to their northern counterparts which increases the ice melt (Azam et al., 2014; Fujita

https://doi.org/10.5194/essd-2022-311
Preprint. Discussion started: 27 September 2022

and Ageta, 2000; Oliphant et al., 2003). Our results (from Sect. 4.3) also show that glaciers having southerly orientation are retreating more than other glaciers, which in turn also supports the above-mentioned ice thickness anomaly.

4.4 Comparison with previous studies in the region

We reemphasize the existing paucity of quality datasets and thereby very few comprehensive studies in the CB Basin. Difference in the time period, datasets and methodologies of these few studies further prevent a thorough intercomparison. Previous studies in the region have also observed a decline in glacier area. Pandey and Venkataraman, (2013) reported a loss of 2.5 % glacier area in the CB Basin during a 30-year time period between 1980 and 2010, overlapping and comparable to the area loss (2.3 %) quantified in the present study. Glacier area in the year 2000 for the selected representative glaciers in their study, (373.1 km^2) and present study (374.64 km^2) are also in agreement. Area in 2000 was found comparable for a study by Sahu and Gupta, (2020) and present study with respect to 5 glaciers they chose for a detailed analysis namely: Gepang Gath (12.7 and 13.40 km^2), Samudra Tapu (80.8 and 81.9 km^2), Bara Shigri (125.1 and 131.5 km^2), Chhota Shigri (14.0 and 15.88 km^2) and Hamtah (3.4 and 3.8 km^2) respectively. Garg et al., (2016) studied 3 glaciers during 1993-2019. Area in 1993 for these glaciers namely: Sakchum (15.61 km^2), Chhota Shigri (15.22 km^2) and Bara Shigri (127.63 km^2) as well as our estimates of 16.04 ± 1.63 km^2, 15.88 ± 0.85 km^2 and 131.50 ± 9.56 km^2 respectively are within a comparable range. The underestimation in area of the Bara Shigri Glacier by Garg et al., (2017) and Sahu and Gupta, (2020) can be attributed to the exclusion of flanks on either side of the glacier which contribute to the glacier flux and have been included in several studies (Chand et al., 2017; Yellala et al., 2019; Nela et al., 2020). The distinctions in glacier boundary defined by different studies contributes further to the challenge of statistical intercomparison and necessitates field surveys and visual inspection in order to ensure accuracy. Therefore, we have carried out various field surveys while also accounting for the following challenges: 1) Nature of the dataset used in the studies. For example, Pandey and Venkataraman, (2013) used Landsat MSS and AWiFS dataset having resolution of 80 and 56 m, respectively, with the co-registration error of 13 and 24 m. The present study has attempted to account for these uncertainties in the glacier inventory by improving on the spatial resolution (viz. Landsat 30 m) and consequently, observed a comparatively lesser rate of glacier area loss. 2) Different methodologies for glacier boundary delineation. While the majority are clean-ice glaciers, several representative glaciers within the study region are debris-covered, making it difficult to differentiate debris from the surrounding topography (Bolch et al., 2008). An automated approach to delineate glacier boundary has more uncertainty in comparison to the manual approach. Manual digitisation carried out in the present study reduces uncertainty as compared to other studies that have opted for a semi-automated approach (viz. Sahu and Gupta, 2020).

With respect to the debris cover area estimation, debris cover change between 1993 and 2014 as estimated by Garg et al., (2017) and present study are comparable with 1.03 and 1.0 ± 0.18 km^2, respectively for Sakchum, 0.45 and 0.71 ± 0.13 km^2, respectively for Chhota Shigri, and 4.82 and 4.94 ± 0.89 km^2, respectively for Bara Shigri. This study is limited to only three glaciers, while the debris cover dataset in our study adds value by way of including 251 glaciers spanning across the CB Basin. In addition to these, the datasets are robust in terms of capturing the glacier dynamics. We find that higher area change is observed in case of south facing glaciers. Our results are in agreement with trends observed in Jankar Chhu watershed by Das and Sharma, (2019) and may be

https://doi.org/10.5194/essd-2022-311
Preprint. Discussion started: 27 September 2022

attributed to the angle of incident solar radiation. South facing glaciers, even in complex local topography are more likely to receive more solar heat available for glacier melting thereby accelerating retreat (Azam et al., 2014; Fujita and Ageta, 2000; Oliphant et al., 2003). Moreover, present glacier inventory (in agreement with Maurer et al., 2016; Sahu and Gupta, 2020) highlights that the Himalayan glaciers with a lake at their snouts are losing mass and shrinking more rapidly than those without (King et al., 2018, 2019), irrespective of debris cover. Calving is an important component of mass loss for a glacier terminating into peri-glacial lake (Maurer et al., 2016; Sakai et al., 2009). We find that area losses for clean ice glaciers as well as glaciers with steeper slopes are higher, as also observed by Sahu and Gupta (2020) and Pandey and Venkataraman (2013). However, in agreement with several other studies on Himalayan glaciers (Chand and Sharma, 2015; Patel et al., 2021; Salerno et al., 2017; Zhao et al., 2020), we do not find a significant correlation between glacier area change and snout elevation in the dataset as a whole. The datasets derived in present study effectively capture the trends observed by previous studies in the region while adding value by way of providing area, debris cover and ice thickness for all glaciers in the basin larger than 0.5 km^2 and also quantifying the uncertainties via robust methodology and extensive field surveys.

5. Data availability and limitations

All three datasets including: 1) inventory of 251 glaciers (> 0.5 km^2) for 1993, 2000, 2010, and 2019; 2) debris cover area for year 1993 and 2019, 3) ice thickness and volume estimates, are available on the Zenodo portal (https://doi.org/10.5281/zenodo.6595546, Vatsal et al., 2022) and include the following files:

1. Glacier inventory: Four shapefiles (.shp) corresponding to year 1993 (glacier_1993.shp), 2000 (glacier_2000.shp), 2010 (glacier_2010.shp) and 2019 (glacier_2019.shp). Shapefiles are widely used file formats supported by open-source GIS softwares. The file attributes include the glacier specific parameters. All outlines are referenced to WGS 84/ UTM Zone 43N.
2. Uncertainty estimation in glacier inventory: 1 (30 m) and ½ (15 m) pixel buffers around the glaciers for year 1993 (buffer_30m_1993.shp and buffer_15m_1993.shp), year 2000 (buffer_30m_2000.shp and buffer_15m_2000.shp), year 2010 (buffer_30m_2010.shp and buffer_15m_2010.shp), and year 2019 (buffer_30m_2019.shp and buffer_15m_2019.shp).
3. Debris cover dataset: Two files in .tiff format corresponding to year 1993 (glacierclass_1993.tif) and 2019 (glacierclass_2019.tif). Each .tiff file contains four different classes namely, ice, snow, debris cover, and ice mix debris.
4. Ice thickness dataset: Single file in .tiff format corresponding to year 2020 (Icethickness.tif).
5. Additional outlines for ease of access: Basin shapefile (CB Basin.shp) and Chandra-Bhaga River shapefile (Chandra Bhaga river.shp).

Manual digitisation as well as on-field surveys for validation have enhanced the robustness of the datasets. However, the users should note that exclusion of glaciers with area < 0.5 km^2 was deemed necessary in order to minimise uncertainty. Nevertheless, the net glacier area is 72 % and 91 % of widely used inventories RGI and GAMDAM, respectively. Studies focused on smaller glaciers can still utilise the datasets to derive valuable information regarding the status of the CB Basin.

6. Conclusion

https://doi.org/10.5194/essd-2022-311
Preprint. Discussion started: 27 September 2022

In the present study, we have generated three major datasets of glaciers in the CB Basin, western Himalaya which quantify spatio-temporal changes between 1993-2019. These datasets include: 1) a homogenous, multi-temporal (1993, 2000, 2010, 2019) glacier inventory of 251 glaciers (> 0.5 km^2), 2) debris cover on each glacier for years 1993 and 2019, and 3) basin-scale ice thickness and glacier volume estimation. The uncertainty associated with the major constraints (snow cover, cloud cover, debris cover, and hill shade) is minimised by performing manual digitisation, and selecting Landsat images of ablation season with minimum cloud cover and desired band combination. For the large-scale debris cover estimation, we have performed maximum likelihood classification within the glacier boundary derived from the inventory, followed by field surveys (with a total of 154 ground validation points) to enhance the accuracy of the dataset. For ice thickness and volume estimation, GlabTop2 model was first tuned for the study area, and thereafter model run was carried out using the glacier inventory and DEMs as input. These DEMs were generated from ASTER L1A stereo pairs using ASP. Model results were validated against GPR-based dataset on 3 representative glaciers in the basin.

We have mapped 251 glaciers with area > 0.5 km^2, which include 216 clean-ice and 35 debris-covered glaciers. 11 glaciers with peri-glacial lake were identified. Total glacierised area showed a continuous reduction: 996 ± 62 km^2 in 1993, 989 ± 68 km^2 in 2000, 982 ± 66 km^2 in 2010 and 973 ± 70 km^2 in 2019. The multidecadal inventory further reveals valuable information regarding the impact of non-climatic factors on glacier area change in the CB Basin: 1) debris-covered glaciers are shrinking at a lesser rate compared to clean-ice glacier, 2) south facing glaciers are losing comparatively more area than other aspects, 3) rate of area loss is higher for glaciers with snout elevation > 5000 m a.s.l., and 4) land-terminating glaciers are more stable than glaciers having peri-glacial lake. Supraglacial debris cover mapping for year 1993 and 2019 shows that debris cover has increased by 14.1 ± 2.54 km^2 during 1993-2019. After accounting for errors due to DEMs and overdeepening, the maximum ice thickness and total volume reserve in the basin is estimated to be 576 ± 45 m and 112.5 ± 41 km^3, respectively for year 2020.

The study summarizes the status of glaciers in the CB Basin by quantifying the glacier area and debris cover changes in the recent decades as well as the ice thickness and volume in the basin. The three sets of spatio-temporal data generated in this study will aid in future research endeavors focusing on glacio-hydrological and policy-based studies as well as contribute towards improving existing inventory information's at both local and regional scales. Also, constant monitoring of glaciers, and further studies into the associated feedback processes is deemed necessary considering the excessive dependence of the downstream population on these glaciers, and the increasing demand for freshwater resources.

7. Author contribution

SV, AB, AM, and MFA conceptualized the study. SV and AM carried out the field work and analysis. SV wrote the manuscript with the guidance of AB, AR, AM, MFA, IMB, NJR and SST, all of whom edited the manuscript and provided valuable suggestions. All authors contributed towards interpretation of result.

8. Competing interests. The authors declare that they have no conflict of interest.

9. Acknowledgements

https://doi.org/10.5194/essd-2022-311
Preprint. Discussion started: 27 September 2022

We are grateful to Space Application Center, Ahmedabad (ISRO) for providing field support under "Integrated studies of Himalayan Cryosphere" programme. We are also thankful to the Glaciology Group, Jawaharlal Nehru University and Hydro-Remote Sensing Applications Group, Department of Civil Engineering, IIT Bombay for providing necessary support for this research. MFA acknowledges the SERB CRG/2020/004478 project.

10. References

Albert, T. H.: Evaluation of Remote Sensing Techniques for Ice-Area Classification Applied to the Tropical for Ice-Area Classification Applied to the Tropical Quelccaya Ice Cap, Peru, Polar Geogr., 26(3), doi:10.1080/789610193, 2002.

Angchuk, T., Ramanathan, A., Bahuguna, I. M., Mandal, A., Soheb, M., Singh, V. B., Mishra, S. and Vatsal, S.: Annual and seasonal glaciological mass balance of Patsio Glacier, western Himalaya (India) from 2010 to 2017, J. Glaciol., doi:10.1017/jog.2021.60, 2021.

Aniya, M., Sato, H., Naruse, R., Skvarca, P. and Casassa, G.: The Use of Satellite and Airborne Imagery to Inventory Outlet Glaciers of the Southern Patagonia Icefield , South America, Photogramm. Eng., 62(12), 1361–1369, 1996.

Azam, M. F., Wagnon, P., Ramanathan, A. L., Vincent, C., Arnaud, Y., Linda, A., Pottakkal, J. G., Chevallier, P., Singh, V.B. and Berthier, E.: From balance to imbalance : a shift in the dynamic behaviour of Chhota Shigri glacier , western Himalaya , India, J. Glaciol., 58(208), 315–324, doi.org/10.3189/2012JoG11J123, 2012.

Azam, M. F., Wagnon, P., Patrick, C., Ramanathan, A., Linda, A. and Singh, V. B.: Reconstruction of the annual mass balance of Chhota Shigri glacier, Western Himalaya, India, since 1969, Ann. Glaciol., 55(66), 69–80, doi:10.3189/2014AoG66A104, 2014.

Azam, M. F., Ramanathan, A. L., Wagnon, P., Vincent, C., Linda, A., Berthier, E., Sharma, P., Mandal, A., Angchuk, T., Singh, V. B. and Pottakkal, J. G.: Meteorological conditions, seasonal and annual mass balances of Chhota Shigri Glacier, western Himalaya, India, Ann. Glaciol., 57(71), 328–338, doi:10.3189/2016AoG71A570, 2016.

Azam, M. F., Wagnon, P., Berthier, E., Vincent, C., Fujita, K. and Kargel, J. S.: Review of the status and mass changes of Himalayan-Karakoram glaciers, J. Glaciol., 64(243), 61–74, doi:10.1017/jog.2017.86, 2018.

Azam, M. F., Kargel, J. S., Shea, J. M., Nepal, S., Haritashya, U. K., Srivastava, S., Maussion, F., Qazi, N., Chevallier, P., Dimri, A. P., Kulkarni, A. V., Cogley, J. G. and Bahuguna, I. M.: Glaciohydrology of the Himalaya-Karakoram, Science ., 3668(June), eabf3668, doi:10.1126/science.abf3668, 2021.

Banerjee, A. and Shankar, R.: On the response of Himalayan glaciers to climate change, J. Glaciol., 59(215), 480–490, doi:10.3189/2013JoG12J130, 2013.

Banerjee, A. and Shankar, R.: Estimating the avalanche contribution to the mass balance of debris covered glaciers, The Cryosphere Discuss., 641–657, doi:10.5194/tcd-8-641-2014, 2014.

Barjacharya, S. R. and Shrestha, B.R.: The status of glaciers in the Hindu Kush–Himalayan region, International

https://doi.org/10.5194/essd-2022-311
Preprint. Discussion started: 27 September 2022

Centre for Integrated Mountain Development, International centre for Integrated Mountain Development (ICIMOD), 1–127, 2011.

Berthier, E., Arnaud, Y., Kumar, R., Ahmad, S., Wagnon, P. and Chevallier, P.: Remote sensing estimates of glacier mass balances in the Himachal Pradesh (Western Himalaya, India), Remote Sens. Environ., 108(3), 327–338, doi:10.1016/j.rse.2006.11.017, 2007.

Bhambri, R. and Bolch, T.: Glacier mapping: a review with special reference to the Indian Himalayas, Prog. Phys. Geogr., 33(5), 672–704, doi:10.1177/0309133309348112, 2009.

Bhambri, R., Bolch, T., Chaujar, R. K. and Kulshreshtha, S. C.: Glacier changes in the Garhwal Himalaya, India, from 1968 to 2006 based on remote sensing, J. Glaciol., 57(203), 543–556, doi:10.3189/002214311796905604, 2011a.

Bhambri, R., Bolch, T., Chaujar, R. K., Kulshreshtha, S. C., Bhambri, R., Bolch, T., Chaujar, R. K. and Kulshreshtha, S. C.: Glacier changes in the Garhwal Himalaya , India , from 1968 to 2006 based on remote sensing Glacier changes in the Garhwal Himalaya , India , from 1968 to 2006 based on remote sensing, J. Glaciol., 57(203), 543–556, DOI: https://doi.org/10.3189/002214311796905604, 2011b.

Bhardwaj, A., Kumar, P., Kumar, M., Sam, L. and Gupta, R. D.: Cold Regions Science and Technology Mapping debris-covered glaciers and identifying factors affecting the accuracy, Cold Reg. Sci. Technol., 106–107, 161–174, https://doi.org/10.1016/j.coldregions.2014.07.006, 2014.

Bhardwaj, A., Joshi, P. K., Snehmani, Sam, L., Singh, M. K., Singh, S. and Kumar, R.: Applicability of Landsat 8 data for characterizing glacier facies and supraglacial debris, Int. J. Appl. Earth Obs. Geoinf., 38, 51–64, doi:10.1016/j.jag.2014.12.011, 2015.

Bhutiyani, M. R., Kale, V. S. and Pawar, N. J.: Long-term trends in maximum, minimum and mean annual air temperature across the Northwwestern Himalaya during the twentieth century, Clim. Change, 85(1-2), 159-177, doi:10.1007/s10584-006-9196-1, 2007.

Bhutiyani, M. R., Kale, V. S. and Pawar, N. J.: Climate change and the precipitation variations in the northwestern Himalaya: 1866-2006, Int. J. Climatol., 30(4), 535–548, doi:10.1002/joc.1920, 2010.

Bliss, A., Hock, R., and Radic, V.: Global response of glacier runoff ´ to twenty-first century climate change, J. Geophys. Res. Earth, 119, 717–730, https://doi.org/10.1002/2013JF002931, 2014.

Bodin, X., Rojas, F. and Brenning, A.: Status and evolution of the cryosphere in the Andes of Santiago (Chile, 33.5°S.), Geomorphology, 118(3–4), 453–464, doi:10.1016/j.geomorph.2010.02.016, 2010.

Bolch, T., Buchroithner, M., Pieczonka, T. and Kunert, A.: Planimetric and volumetric glacier changes in the Khumbu Himal, Nepal, since 1962 using Corona, Landsat TM and ASTER data, J. Glaciol., 54(187), 592–600, doi:10.3189/002214308786570782, 2008.

Bolch, T., Yao, T., Kang, S., Buchroithner, M. F., Scherer, D., Maussion, F., Huintjes, E. and Schneider, C.: A glacier inventory for the western Nyainqentanglha range and the Nam Co Basin, Tibet, and glacier changes 1976-

https://doi.org/10.5194/essd-2022-311
Preprint. Discussion started: 27 September 2022

2009, Cryosphere, 4(3), 419–433, doi:10.5194/tc-4-419-2010, 2010.

Bolch, T., Kulkarni, A., Kääb, A., Huggel, C., Paul, F., Cogley, J. G., Frey, H., Kargel, J. S., Fujita, K., Scheel, M., Bajracharya, S. and Stoffel, M.: The State and Fate of Himalayan Glaciers, Science., 336(6079), 310–314, DOI: 10.1126/science.1215828, 2012.

Bolkas, D., Fotopoulos, G., Braun, A. and Tziavos, I. N.: Assessing Digital Elevation Model Uncertainty Using GPS Survey Data, J. Surv. Eng., 142(3), 1–8, doi:10.1061/(asce)su.1943-5428.0000169, 2016.

Bookhagen, B. and Burbank, D. W.: Toward a complete Himalayan hydrological budget: Spatiotemporal distribution of snowmelt and rainfall and their impact on river discharge, J. Geophys. Res. Earth Surf., 115(3), 1–25, doi:10.1029/2009JF001426, 2010.

Brun, F., Berthier, E., Wagnon, P., Kääb, A. and Treichler, D.: A spatially resolved estimate of High Mountain Asia glacier mass balances from 2000 to 2016, Nat. Geosci., 10(9), 668–673, doi:10.1038/ngeo2999, 2017.

Burger, F., Ayala, A., Farias, D., Shaw, T. E., MacDonell, S., Brock, B., McPhee, J. and Pellicciotti, F.: Interannual variability in glacier contribution to runoff from a high-elevation Andean catchment: understanding the role of debris cover in glacier hydrology, Hydrol. Process., 33(2), 214–229, doi:10.1002/hyp.13354, 2019.

Chand, P. and Sharma, M. C.: Glacier changes in the Ravi basin, North-Western Himalaya (India) during the last four decades (1971-2010/13), Glob. Planet. Change, 135, 133–147, doi:10.1016/j.gloplacha.2015.10.013, 2015.

Chand, P., Sharma, M. C., Bhambri, R., Sangewar, C. V. and Juyal, N.: Reconstructing the pattern of the Bara Shigri Glacier fluctuation since the end of the Little Ice Age, Chandra valley, north-western Himalaya, Prog. Phys. Geogr., 41(5), 643–675, doi:10.1177/0309133317728017, 2017.

Chowdhury, A., Sharma, M.C., Kumar De, S. and Debnath, M.: Glacier changes in the Chhobo Chhu Watershed of the Tista basin between 1975 and 2018, the Sikkim Himalaya, India, Earth Syst. Sci. Data, 13(6), 2923-2944, doi:10.5194/essd-13-2923-2021, 2021.

Cogley, J. G.: Present and future states of Himalaya and Karakoram glaciers, Ann. Glaciol., 52(59), 69–73, doi:10.3189/172756411799096277, 2011.

Colonia, D., Torres, J., Haeberli, W., Schauwecker, S., Braendle, E., Giraldez, C. and Cochachin, A.: Compiling an inventory of glacier-bed overdeepenings and potential new lakes in de-glaciating areas of the peruvian andes: Approach, first results, and perspectives for adaptation to climate Change, Water, 9(5), doi:10.3390/w9050336, 2017.

Das, S. and Sharma, M. C.: Glacier changes between 1971 and 2016 in the Jankar Chhu Watershed, Lahaul Himalaya, India, J. Glaciol., 65(249), 13–28, doi:10.1017/jog.2018.77, 2019.

Dehecq, A., Gourmelen, N., Gardner, A. S., Brun, F., Goldberg, D., Nienow, P. W., Berthier, E., Vincent, C., Wagnon, P. and Trouvé, E.: Twenty-first century glacier slowdown driven by mass loss in High Mountain Asia, Nat. Geosci., 12(1), 22–27, doi:10.1038/s41561-018-0271-9, 2019.

Farinotti, D., Huss, Mölg M., Fürst, J. J., Landmann, J., Machguth, H., Maussion, F. and Pandit, A.: A consensus

https://doi.org/10.5194/essd-2022-311
Preprint. Discussion started: 27 September 2022

estimate for the ice thickness distribution of all glaciers on Earth, Nat. Geosci., 12(3), 168–173, doi:10.1038/s41561-019-0300-3, 2019.

Fitzgerald, R. W. and Lees, B. G.: Assessing the classification accuracy of multisource remote sensing data, Remote Sens. Environ., 47(3), 362–368, doi:10.1016/0034-4257(94)90103-1, 1994.

Frey, H., Paul, F. and Strozzi, T.: Compilation of a glacier inventory for the western Himalayas from satellite data: Methods, challenges, and results, Remote Sens. Environ., 124, 832–843, doi:10.1016/j.rse.2012.06.020, 2012.

Frey, H., Machguth, H., Huss, M., Huggel, C., Bajracharya, S., Bolch, T., Kulkarni, A., Linsbauer, A., Salzmann, N. and Stoffel, M.: Estimating the volume of glaciers in the Himalayan-Karakoram region using different methods, Cryosph., 8(6), 2313–2333, doi:10.5194/tc-8-2313-2014, 2014.

Fujita, K. and Ageta, Y.: Effect of summer accumulation on glacier mass balance on the Tibetan Plateau revealed by mass-balance model, J. Glaciol., 46(153), 244–252, doi:10.3189/172756500781832945, 2000.

Furian, W., Loibl, D. and Schneider, C.: Future glacial lakes in High Mountain Asia: An inventory and assessment of hazard potential from surrounding slopes, J. Glaciol., 67(264), 653–670, doi:10.1017/jog.2021.18, 2021.

Garg, P. K., Shukla, A., Tiwari, R. K. and Jasrotia, A. S.: Assessing the status of glaciers in part of the Chandra basin, Himachal HimalayaA multiparametric approach, Geomorphology, 284, 99–114, doi:10.1016/j.geomorph.2016.10.022, 2017.

Gharehchahi, S., James, W. H. M., Bhardwaj, A., Jensen, J. L. R., Sam, L., Ballinger, T. J. and Butler, D. R.: Glacier ice thickness estimation and future lake formation in swiss southwestern alps—the upper rhône catchment: A VOLTA application, Remote Sens., 12(20), 1–28, doi:10.3390/rs12203443, 2020.

Govt. of HP, 2022: https://agricoop.nic.in/sites/default/files/HP6-Lahaul%20%26%20Spiti-31.12.2012.pdf, last access: 20- February-2022.

Govt. of HP, 2022: https://himachaltourism.gov.in/wp-content/uploads/2019/09/Himachal-Pradesh-Tourism-Policy-2019.pdf, last access: 24- July- 2022.

Granshaw, F. D. and Fountain, A. G.: Glacier change (1958-1998) in the North Cascades National Park Complex, Washington, USA, J. Glaciol., 52(177), 251–256, doi:10.3189/172756506781828782, 2006.

Gratton, D. J., Howarth, P. J. and Marceau, D. J.: Combining DEM Parameters with Landsat MSS and TM Imagery in a GIS for Mountain Glacier Characterization, IEEE Trans. Geosci. Remote Sens., 28(4), 766–769, doi:10.1109/TGRS.1990.573023, 1990.

Haeberli, W. and Hoelzle, M.: Application of inventory data for estimating characteristics of and regional climate-change effects on mountain glaciers: a pilot study with the European Alps, Ann. Glaciol., 21, 206–212, doi:10.3189/s0260305500015834, 1995.

Hall, D. K., Bayr, K. J., Schöner, W., Bindschadler, R. A. and Chien, J. Y. L.: Consideration of the errors inherent in mapping historical glacier positions in Austria from the ground and space (1893-2001), Remote Sens. Environ.,

https://doi.org/10.5194/essd-2022-311
Preprint. Discussion started: 27 September 2022

86(4), 566–577, doi:10.1016/S0034-4257(03)00134-2, 2003.

Hannah, D. M., Gurnell, A. M. and McGregor, G. R.: Spatio-temporal variation in microclimate, the surface energy balance and ablation over a cirque glacier, Int. J. Climatol., 20(7), 733–758, doi:10.1002/1097-0088(20000615)20:7<733::AID-JOC490>3.0.CO;2-F, 2000.

Herreid, S., Pellicciotti, F., Ayala, A., Chesnokova, A., Kienholz, C., Shea, J. and Shrestha, A.: Satellite observations show no net change in the percentage of supraglacial debris-covered area in northern Pakistan from 1977 to 2014, J. Glaciol., 61(227), 524–536, doi:10.3189/2015JoG14J227, 2015.

Holobâcă, I. H., Tielidze, L. G., Ivan, K., Elizbarashvili, M., Alexe, M., Germain, D., Petrescu, S. H., Pop, O. T. and Gaprindashvili, G.: Multi-sensor remote sensing to map glacier debris cover in the Greater Caucasus, Georgia, J. Glaciol., doi:10.1017/jog.2021.47, 2021.

Huss, M. and Hock, R.: A new model for global glacier change and sea-level rise, Front. Earth Sci., 3, 34, https://doi.org/10.3389/feart.2015.00054, 2015.

Immerzeel, W. W., van Beek, L. P. H. and Bierkens, M. F. P.: Climate Change Will Affect the Asian Water Towers, Science., 328(5984), 1382 LP – 1385, doi:10.1126/science.1183188, 2010.

Immerzeel, W. W., Lutz, A. F., Andrade, M., Bahl, A., Biemans, H., Bolch, T., Hyde, S., Brumby, S., Davies, B. J., Elmore, A. C., Emmer, A., Feng, M., Fernández, A., Haritashya, U., Kargel, J. S., Koppes, M., Kraaijenbrink, P. D. A., Kulkarni, A. V., Mayewski, P. A., Nepal, S., Pacheco, P., Painter, T. H., Pellicciotti, F., Rajaram, H., Rupper, S., Sinisalo, A., Shrestha, A. B., Viviroli, D., Wada, Y., Xiao, C., Yao, T. and Baillie, J. E. M.: Importance and vulnerability of the world's water towers, Nature, 577(7790), 364–369, doi:10.1038/s41586-019-1822-y, 2020.

Janke, J. R., Bellisario, A. C. and Ferrando, F. A.: Classification of debris-covered glaciers and rock glaciers in the Andes of central Chile, Geomorphology, 241, 98–121, doi:10.1016/j.geomorph.2015.03.034, 2015.

Janssen, L. L. F. and van der Wel, F. J. M.: Accuracy assessment of satellite derived land- cover data: A review, Photogramm. Eng. Remote Sensing, 60(4), 419–426, 1994.

Jreat, Manoj. Tourism in Himachal Pradesh. Indus Publishing, 2004.

Kääb, A., Paul, F., Maisch, M., Hoelzle, M. and Haeberli, W.: The new remote-sensing-derived Swiss glacier inventory: II. First results, Ann. Glaciol., 34(September 1985), 362–366, doi:10.3189/172756402781817473, 2002.

Kääb, A., Berthier, E., Nuth, C., Gardelle, J. and Arnaud, Y.: Contrasting patterns of early twenty-first-century glacier mass change in the Himalayas, Nature, 488(7412), 495–498, doi:10.1038/nature11324, 2012a.

Kääb, A., Berthier, E., Nuth, C., Gardelle, J. and Arnaud, Y.: Contrasting patterns of early twenty-first-century glacier mass change in the Himalayas, Nature, 488(7412), 495–498, doi:10.1038/nature11324, 2012b.

Kashyap, H. and Parsheera, C.M.: Sustainable economic development of Himachal Pradesh through small hydro power prject, Conflu. Knowl., 4(1), 69-75, 2016.

https://doi.org/10.5194/essd-2022-311
Preprint. Discussion started: 27 September 2022

King, O., Dehecq, A., Quincey, D. and Carrivick, J.: Contrasting geometric and dynamic evolution of lake and land-terminating glaciers in the central Himalaya, Glob. Planet. Change, 167, 46–60, doi:10.1016/j.gloplacha.2018.05.006, 2018.

King, O., Bhattacharya, A., Bhambri, R. and Bolch, T.: Glacial lakes exacerbate Himalayan glacier mass loss, Sci. Rep., 9(1), 1–9, doi:10.1038/s41598-019-53733-x, 2019.

Koul, M. N. and Ganjoo, R. K.: Impact of inter- and intra-annual variation in weather parameters on mass balance and equilibrium line altitude of Naradu Glacier (Himachal Pradesh), NW Himalaya, India, Clim. Change, 99(1), 119–139, doi:10.1007/s10584-009-9660-9, 2010.

Kraaijenbrink, P. D. A., Bierkens, M. F. P., Lutz, A. F. and Immerzeel, W. W.: Impact of a global temperature rise of 1.5 degrees Celsius on Asia's glaciers, Nature, 549(7671), 257–260, doi:10.1038/nature23878, 2017.

Kulkarni, A. V., Rathore, B. P., Singh, S. K. and Bahuguna, I. M.: Understanding changes in the Himalayan cryosphere using remote sensing techniques, Int. J. Remote Sens., 32(3), 601–615, doi:10.1080/01431161.2010.517802, 2011.

Kumar, A., Mishra, R., Singh, D., Pramanik, S., Prakash, O., Mukhtar, A., Mohan, M., Kumar, P., Shukla, S. P.: Long term monitoring of mass balance of Hamtah Glacier, Lahaul and Spiti District, Himachal Pradesh - On expedition basis, Geol. Surv. India, 147, 230–231, 2016.

Kumari, S., Pandit, A., Ramsankaran, R., Soheb, M., Angchuk, T. and Ramanathan, A. L.: Modelling ice thickness distribution and volume of Patsio Glacier in Western Himalayas, J. Earth Syst. Sci., 130(3), doi:10.1007/s12040-021-01643-w, 2021.

Li, F., Maussion, F., Wu, G., Chen, W., Yu, Z., Li, Y. and Liu, G.: Influence of glacier inventories on ice thickness estimates and future glacier change projections in the Tian Shan range , Central Asia, J. Glaciol., 1–15, DOI: https://doi.org/10.1017/jog.2022.60 2022.

Li, H., Haugen, J. E. and Xu, C. Y.: Precipitation pattern in the Western Himalayas revealed by four datasets, Hydrol. Earth Syst. Sci., 22(10), 5097–5110, doi:10.5194/hess-22-5097-2018, 2018.

Linsbauer, A., Frey, H., Haeberli, W., Machguth, H., Azam, M. F. and Allen, S.: Modelling glacier-bed overdeepenings and possible future lakes for the glaciers in the Himalaya-Karakoram region, Ann. Glaciol., 57(71), 119–130, doi:10.3189/2016AoG71A627, 2016.

Mandal, A., Ramanathan, A., Azam, M. F., Angchuk, T., Soheb, M., Kumar, N., Pottakkal, J. G., Vatsal, S., Mishra, S. and Singh, V. B.: Understanding the interrelationships among mass balance, meteorology, discharge and surface velocity on Chhota Shigri Glacier over 2002-2019 using in situ measurements, J. Glaciol., 66(259), 727–741, doi:10.1017/jog.2020.42, 2020.

Massuel, S., Feurer, D., El Maaoui, M. A. and Calvez, R.: Deriving bathymetries from unmanned aerial vehicles: a case study of a small intermittent reservoir, Hydrol. Sci. J., 67(1), 82–93, doi:10.1080/02626667.2021.1988614, 2022.

https://doi.org/10.5194/essd-2022-311
Preprint. Discussion started: 27 September 2022

Maurer, J. M., Rupper, S. B. and Schaefer, J. M.: Quantifying ice loss in the eastern Himalayas since 1974 using declassified spy satellite imagery, Cryosphere, 10(5), 2203–2215, doi:10.5194/tc-10-2203-2016, 2016.

Mohd Hasmadi, I. and Kamaruzam, J.: Satellite data classification accuracy assessment based from reference dataset, Int. J. Comput. Inf. Sci. Eng., 2(2), 96–102, Available from: http://www.waset.org/ijcise/v2/v2-2-16.pdf , 2008.

Mölg, N., Bolch, T., Rastner, P., Strozzi, T. and Paul, F.: A consistent glacier inventory for Karakoram and Pamir derived from Landsat data: Distribution of debris cover and mapping challenges, Earth Syst. Sci. Data, 10(4), 1807–1827, doi:10.5194/essd-10-1807-2018, 2018.

Nela, B. R., Singh, G., Bandyopadhyay, D., Patil, A., Mohanty, S., Musthafa, M. and Dasondhi, G.: Estimating Dynamic Parameters of Bara Shigri Glacier and Derivation of Mass Balance from Velocity, Int. Geosci. Remote Sens. Symp., 3002–3005, doi:10.1109/IGARSS39084.2020.9323152, 2020.

Nuimura, T., Sakai, A., Taniguchi, K., Nagai, H., Lamsal, D., Tsutaki, S., Kozawa, A., Hoshina, Y., Takenaka, S., Omiya, S., Tsunematsu, K., Tshering, P. and Fujita, K.: The GAMDAM glacier inventory: A quality-controlled inventory of Asian glaciers, Cryosphere, 9(3), 849–864, doi:10.5194/tc-9-849-2015, 2015.

Nuth, C. and Kääb, A.: Co-registration and bias corrections of satellite elevation data sets for quantifying glacier thickness change, The Cryosphere, 5, 271–290, https://doi.org/10.5194/tc-5-271-2011, 2011.

Oliphant, A. J., Spronken-Smith, R. A., Sturman, A. P. and Owens, I. F.: Spatial variability of surface radiation fluxes in mountainous terrain, J. Appl. Meteorol., 42(1), 113–128, doi:10.1175/1520-0450(2003)042<0113:SVOSRF>2.0.CO;2, 2003.

Pandey, P. and Venkataraman, G.: Changes in the glaciers of Chandra-Bhaga basin, Himachal Himalaya, India, between 1980 and 2010 measured using remote sensing, Int. J. Remote Sens., 34(15), 5584–5597, doi:10.1080/01431161.2013.793464, 2013.

Pandey, V. K., Mishra, A. and Mishra, S. S.: Climate Change And Mitigation Measures For The Hydrometerological Disaster In Himachal Pradesh , India- In Light Of Dams, Int. J. Sci. Technol. Res., 4(01), 267–276, 2015.

Pandey, P., Ali, S. N., Ramanathan, A. L., Champati ray, P. K. and Venkataraman, G.: Regional representation of glaciers in Chandra Basin region, western Himalaya, India, Geosci. Front., 8(4), 841–850, doi:10.1016/j.gsf.2016.06.006, 2017.

Pandit, A. and Ramsankaran, R.: Modeling ice thickness distribution and storage volume of glaciers in Chandra Basin, western Himalayas, J. Mt. Sci., 17(8), 2011–2022, doi:10.1007/s11629-019-5718-y, 2020.

Patel, L. K., Sharma, A., Sharma, P., Singh, A. and Thamban, M.: Glacier area changes and its relation to climatological trends over Western Himalaya between 1971 and 2018, J. Earth Syst. Sci., 130(4), doi:10.1007/s12040-021-01720-0, 2021.

Paul, F.: Evaluation of different methods for glacier mapping using landsat TM, EARSeL eProceedings 1, no. 1,

https://doi.org/10.5194/essd-2022-311
Preprint. Discussion started: 27 September 2022

239-245 , 2000.

Paul, F., Kääb, A., Maisch, M., Kellenberger, T. and Haeberli, W.: The new remote-sensing derived Swiss glacier inventory. 1. Methods, Ann. Glaciol., 34(September 1985), 355–361, doi:10.3189/172756402781817941, 2002.

Paul, F., Huggel, C. and Kääb, A.: Combining satellite multispectral image data and a digital elevation model for mapping debris-covered glaciers, Remote Sens. Environ., 89(4), 510–518, doi:10.1016/j.rse.2003.11.007, 2004.

Paul, F., Barrand, N. E., Baumann, S., Berthier, E., Bolch, T., Casey, K., Frey, H., Joshi, S. P., Konovalov, V., Le Bris, R., Mölg, N., Nosenko, G., Nuth, C., Pope, A., Racoviteanu, A., Rastner, P., Raup, B., Scharrer, K., Steffen, S. and Winsvold, S.: On the accuracy of glacier outlines derived from remote-sensing data, Ann. Glaciol., 54(63), 171–182, doi:10.3189/2013AoG63A296, 2013.

Paul, F., Bolch, T., Kääb, A., Nagler, T., Nuth, C., Scharrer, K., Shepherd, A., Strozzi, T., Ticconi, F., Bhambri, R., Berthier, E., Bevan, S., Gourmelen, N., Heid, T., Jeong, S., Kunz, M., Lauknes, T. R., Luckman, A., Merryman Boncori, J. P., Moholdt, G., Muir, A., Neelmeijer, J., Rankl, M., VanLooy, J. and Van Niel, T.: The glaciers climate change initiative: Methods for creating glacier area, elevation change and velocity products, Remote Sens. Environ., 162, 408–426, doi:10.1016/j.rse.2013.07.043, 2015.

Paul, F., Bolch, T., Briggs, K., Kääb, A., McMillan, M., McNabb, R., Nagler, T., Nuth, C., Rastner, P., Strozzi, T. and Wuite, J.: Error sources and guidelines for quality assessment of glacier area, elevation change, and velocity products derived from satellite data in the Glaciers_cci project, Remote Sens. Environ., 203(November 2016), 256–275, doi:10.1016/j.rse.2017.08.038, 2017.

Pfeffer, W. T., Arendt, A. A., Bliss, A., Bolch, T., Cogley, J. G., Gardner, A. S., Hagen, J.-O., Hock, R., Kaser, G., Kienholz, C., Miles, E. S., Moholdt, G., Mölg, N., Paul, F., Radic, V., Rastner, ´ P., Raup, B. H., Rich, J., and Sharp, M. J.: The Randolph Glacier Inventory: A globally complete inventory of glaciers, J. Glaciol., 60, 537–552, https://doi.org/10.3189/2014JoG13J176, 2014.

Prakash, C. and Nagarajan, R.: Outburst susceptibility assessment of moraine-dammed lakes in Western Himalaya using an analytical hierarchy process, Earth Surf. Process. Landforms, 42(14), 2306-2321, doi:10.1002/esp.4185, 2017.

Prakash, S., Sharma, M. C., Shahnawaz, Pandey, V. K., Chand, P. and Deswal, S.: Mapping Glacial Geomorphology and Livelihood Resources in Urgos Watershed, Lahul and Spiti District, Himachal Pradesh, India, J. Indian Soc. Remote Sens., 47(8), 1295–1305, doi:10.1007/s12524-019-01002-9, 2019.

Pratap, B., Dobhal, D. P., Bhambri, R., Mehta, M. and Tewari, V. C.: Four decades of glacier mass balance observations in the Indian Himalaya, Reg. Environ. Chang., 16(3), 643–658, doi:10.1007/s10113-015-0791-4, 2016.

Preety, K., Prasad, A. K., Varma, A. K. and El-Askary, H.: Accuracy Assessment, Comparative Performance, and Enhancement of Public Domain Digital Elevation Models (ASTER 30 m, SRTM 30 m, CARTOSAT 30 m, SRTM 90 m, MERIT 90 m, and TanDEM-X 90 m) Using DGPS, Remote Sens., 14(6), doi:10.3390/rs14061334, 2022.

Racoviteanu, A. E., Arnaud, Y., Williams, M. W. and Ordoñez, J.: Decadal changes in glacier parameters in the

https://doi.org/10.5194/essd-2022-311
Preprint. Discussion started: 27 September 2022

Cordillera Blanca, Peru, derived from remote sensing, J. Glaciol., 54(186), 499–510, doi:10.3189/002214308785836922, 2008.

Ramsankaran, R., Pandit, A. and Azam, M. F.: Spatially distributed ice-thickness modelling for Chhota Shigri Glacier in western Himalayas, India, Int. J. Remote Sens., 39(10), 3320–3343, doi:10.1080/01431161.2018.1441563, 2018.

Rawat, Y. S., Vishvakarma, S.C., Oinam, S. S. and Kuniyal, J.C.: Diversity, distribution and vegetation assessment in the Jahlmanal watershed in cold desert of the Lahaul valley, north-western Himalaya, India, IForest-Biogeosciences and Forestry, 3(May), 65-71, doi:10.3832/ifor0532-003, 2010.

RGI Consortium, 2017. Randolph Glacier Inventory - A Dataset of Global Glacier Outlines, Version 6. [Indicate subset used]. Boulder, Colorado USA. NSIDC: National Snow and Ice Data Center. doi: https://doi.org/10.7265/4m1f-gd79.

Rounce, D. R., Hock, R., McNabb, R. W., Millan, R., Sommer, C., Braun, M. H., Malz, P., Maussion, F., Mouginot, J., Seehaus, T. C. and Shean, D. E.: Distributed Global Debris Thickness Estimates Reveal Debris Significantly Impacts Glacier Mass Balance, Geophys. Res. Lett., 48(8), doi:10.1029/2020GL091311, 2021.

Sahu, R. and Gupta, R. D.: Glacier mapping and change analysis in Chandra basin , Western Himalaya , India during 1971 – 2016, Int. J. Remote Sens., 41(18), 6914–6945, doi:10.1080/01431161.2020.1752412, 2020.

Sakai, A.: Brief Communication: Updated GAMDAM Glacier Inventory over the High Mountain Asia, Cryosph. Discuss., 1–12, doi:10.5194/tc-2018-139, 2018.

Sakai, A., Nishimura, K., Kadota, T. and Takeuchi, N.: Onset of calving at supraglacial lakes on debris-covered glaciers of the Nepal Himalaya, J. Glaciol., 55(193), 909–917, doi:10.3189/002214309790152555, 2009.

Salerno, F., Thakuri, S., Tartari, G., Nuimura, T., Sunako, S., Sakai, A. and Fujita, K.: Debris-covered glacier anomaly? Morphological factors controlling changes in the mass balance, surface area, terminus position, and snow line altitude of Himalayan glaciers, Earth Planet. Sci. Lett., 471, 19–31, doi:10.1016/j.epsl.2017.04.039, 2017.

Sam, L., Bhardwaj, A., Singh, S. and Kumar, R.: Remote sensing flow velocity of debris-covered glaciers using Landsat 8 data, Prog. Phys. Geogr., 40(2), 305–321, doi:10.1177/0309133315593894, 2016.

Sam, L., Bhardwaj, A., Kumar, R., Buchroithner, M. F. and Martín-Torres, F. J.: Heterogeneity in topographic control on velocities of Western Himalayan glaciers, Sci. Rep., 8(1), 1–16, doi:10.1038/s41598-018-31310-y, 2018.

Schauwecker, S., Rohrer, M., Huggel, C., Kulkarni, A., Ramanathan, A. L., Salzmann, N., Stoffel, M. and Brock, B.: Remotely sensed debris thickness mapping of Bara Shigri Glacier, Indian Himalaya, J. Glaciol., 61(228), 675–688, doi:10.3189/2015JoG14J102, 2015.

Scherler, D., Bookhagen, B. and Strecker, M. R.: Spatially variable response of Himalayan glaciers to climate change affected by debris cover, Nat. Geosci., 4(3), 156–159, doi:10.1038/ngeo1068, 2011a.

https://doi.org/10.5194/essd-2022-311
Preprint. Discussion started: 27 September 2022

Scherler, D., Bookhagen, B. and Strecker, M. R.: Hillslope-glacier coupling: The interplay of topography and glacial dynamics in High Asia, J. Geophys. Res. Earth Surf., 116(2), 1–21, doi:10.1029/2010JF001751, 2011b.

Setianto, A. and Triandini, T.: Comparison of Kriging and Inverse Distance Weighted (IDW) Interpolation Methods in Lineament Extraction and Analysis, J. Appl. Geol., 5(1), 21–29, doi:10.22146/jag.7204, 2015.

Sharma, P., Patel, L. K., Ravindra, R., Singh, A., Mahalinganathan, K. and Thamban, M.: Role of debris cover to control specific ablation of adjoining batal and sutri dhaka glaciers in chandra basin (Himachal Pradesh) during peak ablation season, J. Earth Syst. Sci., 125(3), 459–473, doi:10.1007/s12040-016-0681-2, 2016.

Shean, D. E., Alexandrov, O., Moratto, Z. M., Smith, B. E., Joughin, I. R., Porter, C. and Morin, P.: An automated, open-source pipeline for mass production of digital elevation models (DEMs) from very-high-resolution commercial stereo satellite imagery, ISPRS J. Photogramm. Remote Sens., 116(206), 101–117, doi:10.1016/j.isprsjprs.2016.03.012, 2016.

Shean, D. E., Bhushan, S., Montesano, P., Rounce, D. R., Arendt, A. and Osmanoglu, B.: A Systematic, Regional Assessment of High Mountain Asia Glacier Mass Balance, Front. Earth Sci., 7(February), doi:10.3389/feart.2019.00363, 2020.

Shekhar, M., Bhardwaj, A., Singh, S., Ranhotra, P. S., Bhattacharyya, A., Pal, A. K., Roy, I., Martín-Torres, F. J. and Zorzano, M. P.: Himalayan glaciers experienced significant mass loss during later phases of little ice age, Sci. Rep., 7(1), 1–14, doi:10.1038/s41598-017-09212-2, 2017.

Shukla, A., Gupta, R. P. and Arora, M. K.: Estimation of debris cover and its temporal variation using optical satellite sensor data: A case study in Chenab basin, Himalaya, J. Glaciol., 55(191), 444–452, doi:10.3189/002214309788816632, 2009.

Shukla, A. and Garg, P. K.: Evolution of a debris-covered glacier in the western Himalaya during the last four decades (1971–2016): A multiparametric assessment using remote sensing and field observations, Geomorphology, 341, 1–14, doi:10.1016/j.geomorph.2019.05.009, 2019.

Shukla, A., Garg, S., Mehta, M., Kumar, V. and Kant Shukla, U.: Temporal inventory of glaciers in the Suru sub-basin, western Himalaya: Impacts of regional climate variability, Earth Syst. Sci. Data, 12(2), 1245–1265, doi:10.5194/essd-12-1245-2020, 2020.

Sidjak, R. W. and Wheate, R. D.: Glacier mapping of the Illecillewaet icefield, British Columbia, Canada, using Landsat TM and digital elevation data, Int. J. Remote Sens., 20(2), 273–284, doi:10.1080/014311699213442, 1999.

Singh, P., Jain, S. K. and Kumar, N.: Estimation of Snow and Glacier-Melt Contribution to the Chenab River, Western Himalaya, Mountain Research and Development., 17(1), 49–56, Stable URL: http://www.jstor.org/stable/3673913, 1997.

Singh, S., Kumar, R., Bhardwaj, A., Sam, L., Shekhar, M., Singh, A., Kumar, R. and Gupta, A.: Changing climate and glacio-hydrology in Indian Himalayan Region: A review, Wiley Interdiscip. Rev. Clim. Chang., 7(3), 393–410, doi:10.1002/wcc.393, 2016.

https://doi.org/10.5194/essd-2022-311
Preprint. Discussion started: 27 September 2022

South Asia Network on Dams, River & People: https://sandrp.files.wordpress.com/2018, last access: 12 July 2022.

Swain, A. K., Mukhtar, M. A., Majeed, Z. and Shukla, S. P.: Depth profiling and recessional history of the Hamtah and Parang glaciers in Lahaul and Spiti, Himachal Pradesh, Indian Himalaya, Geol. Soc. Spec. Publ., 462(1), 35–49, doi:10.1144/SP462.11, 2018.

Tawde, S. A., Kulkarni, A. V and Bala, G.: An estimate of glacier mass balance for the Chandra basin, western Himalaya, for the period 1984-2012, Ann. Glaciol., 58(75), 99–109, doi:10.1017/aog.2017.18, 2017.

Vatsal, S., Bhardwaj, A., Azam, M. F., Mandal, A., Ramanathan, A., Bahuguna, I. M., Raju, N. J. and Tomar, S. S.: Glacier_inventory_debris_cover_ice_thickness_dataset_Chandra_Bhaga_basin_Himalaya, *ZENODO*, doi:10.5281/ZENODO.6595546, 2022.

Vaughan, D. G., Comiso, J. C., Allison, I., Carrasco, J., Kaser, G., Kwok, R., Mote, P., Murray, T., Paul, F., Ren, J., Rignot, E., Solomina, O., Steffen, K., and Zhang, T.: Observations: Cryosphere, in: Climate Change 2013: Physical Science Basis. Contribution of Working Group I to the Fifth Assessment Report of the Intergovernmental Panel on Climate Change, edited by: Stocker, T. F., Qin, D., Plattner, G.-K., Tignor, M., Allen, S. K., Boschung, J., Nauels, A., Xia, Y., Bex, V., and Midgley, P. M., Cambridge University Press, Cambridge, United Kingdom and New York, NY, USA, 2013.

Vijay, S. and Braun, M.: Elevation change rates of glaciers in the Lahaul-Spiti (Western Himalaya, India) during 2000-2012 and 2012-2013, Remote Sens., 8(12), 1–16, doi:10.3390/rs8121038, 2016.

Viviroli, D., Archer, D. R., Buytaert, W., Fowler, H. J., Greenwood, G. B., Hamlet, A. F., Huang, Y., Koboltschnig, G., Litaor, M. I., López-Moreno, J. I., Lorentz, S., Schädler, B., Schreier, H., Schwaiger, K., Vuille, M. and Woods, R.: Climate change and mountain water resources: Overview and recommendations for research, management and policy, Hydrol. Earth Syst. Sci., 15(2), 471–504, doi:10.5194/hess-15-471-2011, 2011.

Wagner, T., Pauritsch, M., Mayaud, C., Kellerer-Pirklbauer, A., Thalheim, F. and Winkler, G.: Controlling factors of microclimate in blocky surface layers of two nearby relict rock glaciers (Niedere Tauern Range, Austria), Geogr. Ann. Ser. A Phys. Geogr., 101(4), 310–333, doi:10.1080/04353676.2019.1670950, 2019.

Wagnon, P., Linda, A., Arnaud, Y., Kumar, R., Sharma, P., Vincent, C., Pottakkal, J. G., Berthier, E., Ramanathan, A., Hasnain, S. I. and Chevallier, P.: Four years of mass balance on Chhota Shigri Glacier , Himachal Pradesh , India , a new benchmark glacier in the western Himalaya, , 53(183), 603–611, 2007.

Wang, Y., Hou, S. and Liu, Y.: Glacier changes in the Karlik Shan, eastern Tien Shan, during 1971/72-2001/02, Ann. Glaciol., 50(53), 39–45, doi:10.3189/172756410790595877, 2009.

Winston, Y., Yang, Chen, Y., Savitsky, A., Alford, D., Brown, C., Wescoat, J., Debowicz, D. and Robinson, S.: Hydrology and Glaciers in the Upper Indus Basin, in: The impact of Climate Risks on Water and Agriculture, 57-76, https://doi.org/10.1596/9780821398746_CH03, 2013.

Yellala, A., Kumar, V. and Høgda, K. A.: Bara Shigri and Chhota Shigri glacier velocity estimation in western Himalaya using Sentinel-1 SAR data, Int. J. Remote Sens., 40(15), 5861–5874, doi:10.1080/01431161.2019.1584685, 2019.

https://doi.org/10.5194/essd-2022-311
Preprint. Discussion started: 27 September 2022

Zalazar, L., Ferri, L., Castro, M., Gargantini, H., Gimenez, M., Pitte, P., Ruiz, L., Masiokas, M., Costa, G. and Villalba, R.: Spatial distribution and characteristics of Andean ice masses in Argentina: Results from the first National Glacier Inventory, J. Glaciol., 66(260), 938–949, doi:10.1017/jog.2020.55, 2020.

Zhang, D., Yao, X., Duan, H., Liu, S., Guo, W., Sun, M. and Li, D.: A new automatic approach for extracting glacier centerlines based on Euclidean allocation, Cryosphere, 15(4), 1955–1973, doi:10.5194/tc-15-1955-2021, 2021.

Zhao, X., Wang, X., Wei, J., Jiang, Z., Zhang, Y. and Liu, S.: Spatiotemporal variability of glacier changes and their controlling factors in the Kanchenjunga region, Himalaya based on multi-source remote sensing data from 1975 to 2015, Sci. Total Environ., 745, 140995, doi:10.10fgratto16/j.scitotenv.2020.140995, 2020.

Zou, X., Gao, H., Zhang, Y., Ma, N., Wu, J. and Farhan, S. Bin: Quantifying ice storage in upper Indus river basin using ground-penetrating radar measurements and glacier bed topography model version 2, Hydrol. Process., 35(4), 1–14, doi:10.1002/hyp.14145, 2021.